Application of digester-sludge based biochar on ammonia nitrogen removal

by

Yao Tang

A thesis submitted in partial fulfillment of the requirements for the degree of

Master of Science
in
Environmental Engineering

Department of Civil and Environmental Engineering
University of Alberta

© Yao Tang, 2017

Abstract:

Water contamination by ammonium ions presents huge risks to the ecosystems. This work evaluated the potential application of digested sludge pyrolyzed biochar on ammonium removal. Anaerobic digester sludge was collected from a municipal wastewater treatment plant in Alberta, Canada and pyrolyzed separately from 350 ℃ to 550 ℃ with 50 ℃ temperature interval. The characteristics of biochar were analyzed by elemental analysis, scanning electron microscopy (SEM), BET surface area analysis, and fourier transform infrared spectroscopy (FTIR). It was observed that the biochar yield decreased with an increase in the pyrolysis temperature. Biochar produced at 450℃ (BC450) had the highest ammonium remval capacity due to the incereased surface area and function groups. The Langmuir isotherm best described the relation between digested sludge biochar and ammonium removal capacity at the equilibrium point, indicating that monolayer chemical adsorption was the dominating mechanism. Biochar ammonium removal capacity was 1.2mg NH_4-N/g biochar in municipal wastewater, which is lower than that in the synthetic ammonium solution (1.4 mg NH_4-N/g biochar). Our results demonstrate that the digester sludge biochar is a promising adsorbent for ammonium removal.

Aiming to enhance the biochar ammonium removal capacity, biochar-alginate beads were introduced. By combined sodium alginate as the other kind of supporting material with biochar powder under previous treatment condition, biochar-alginate beads were formatted. Based on ammonium adsorption experiment, 1.5% (w/w) of sodium alginate was the optimal concentration of formatting beads and ammonium adsorption. 3% (w/w) of biochar powder concentration was selected as the best concentration of biochar-alginate beads, which enhanced biochar-alginate beads the ammonium capacity increase about 15% from 2.38 mg/g to 2.74 mg/g. The FTIR results also showed that compared to alginate beads and biochar powder alone, the acidic and oxygen

surface functional groups have enhanced after the biochar-alginate beads were formatted, which were two important functional groups for ammonium adsorption. Mass transfer and mechanical property results showed that biochar-alginate beads are able to transfer nutrients inside and have better resistance under hash operation condition. After bacteria was imbedded inside biochar-alginate beads, a change of mechanism was observed after 24 hours' contact time, which indicated that only the adsorbents remove ammonium from aqueous system rather than bacteria gets involved. The 72 hours' contact time adsorption results showed that biochar-alginate beads imbedded with bacteria were able to uptake 75% of total ammonium. The results indicated biochar-alginate beads can provide a suitable condition for bacterial growth and able to transport nutrients and contaminants inside biochar-alginate beads. Thus, the biochar-alginate beads, the system combined with physisorption, chemisorption and biological removal were established and ready for the further experiments.

Keywords: ammonia, adsorption, biochar, digested sludge, pyrolysis, biochar-alginate, bacteria immobilization

Acknowledgment:

I would like to pay special thankfulness, warmth and appreciation to the persons below who made my research successful and assisted me at every point to cherish my goal:

My Supervisor, Professor Yang Liu, who supported me at every bit and without whom it was impossible to accomplish the end task.

Visiting scholar, Dr. Weijun Tian, who assisted me on experimental design.

Md Samrat from Dr. Daniel Alessi's group with potentiometric titrations analysis.

Kingsley Nze, Stanley Poon, Rachel Yee and all Dr. Liu's group members, whose advise on my research and my thesis.

My Mom, Dad and all the family members, friends, whose unyielding support.

Table of Contents

List of figures:

List of tables:

Chapter 1. Introduction

1. Biochar powder

Ammonia nitrogen (NH_4-N) is the main pollutant in the water system, influencing water potability and causing eutrophication (Li & Liu, 2009; Yang et al., 2007). Ammonia (NH_3) is a potential threat to fish through protein metabolism inhibation (Stuart M. Levit, 2010). Ammonium ion (NH_4^+) decreases dissolved oxygen through nitrification (Ahn et al., 2011). The biological nutrient removal process (BNR) is the most common process worldwide to treat the ammonia nitrogen in municipal wastewater (Ekama & Wentzel, 1999). Anaerobic digester sludge (biosolids), generated at the municipal wastewater treatment, are often disposed of in landfill, in the ocean, or by incineration (Lu et al., 2013), which may lead to human health risks and environmental pollution (Bright & Healey, 2003). However, organic matter and nutrients contained in these biosolids can be retained and converted into value-added products such as biochar, avoiding the environmental and economic costs of disposal.

Recent studies have demonstrated that biochar produced from solid wastes can be a good source of adsorbent. In particular, organic materials such as wood chips (Veksha et al., 2014), coconut shells (Cazetta et al., 2011) and bamboo (Fan et al., 2010), and inorganic cellular materials, such as coal cinder (Y. M. Wang et al., 2016) can be converted to biochar through pyrolysis (Bridle & Pritchard, 2004; Hospido et al., 2005; Strezov & Evans, 2009). During pyrolysis, the high organic content of such waste is transformed and fixed as carbon. Previous studies on the sludge-derived biochar activation process revealed that the raw material and the pyrolysis temperature are the main factors influencing biochar quality and quantity (Smith et al., 2009). Thermal decomposition of sludge material under high temperature leads to transport and phase-out of non-carbon elements as volatile compounds (Goyal et al., 2001), which also

accelerates bonding of freed carbon atoms as elementary graphitic crystallites (Smith et al., 2009). The interstices between the crystallites propagate a rudimentary porous structure, increasing the porosity and enhancing adsorption properties. (Goyal et al., 2001).

Biosolids-derived biochars have been found to effectively adsorb contaminants of great environmental concerns, such as heavy metals (Pb (II), Cr (II), and As (V)) (H. Jin et al., 2014; Zhou et al., 2015), dyes (Silva et al., 2016), phenol and phenolic compounds, and other large organics from wastewater systems (Kacan, 2016; Shi et al., 2014; Yao et al., 2013). Digested sludge can be heated at high temperatures to form biochars that have relatively high microporosity, high surface area (Jindarom et al., 2007), high ion exchange capacity, and various surface chemical functional groups (Chen et al., 2002), which makes them good adsorbents of contaminants, but also natural bacterial carriers. Only one research (Carey et al., 2015) focus on the application of biosolids-derived biochar on ammonium removal from different ammonium concentration solution and turfgrass cultivation, however none papers evaluated the effect of pyrolysis temperature on sludge-based biochar ammonium removal from municipal wastewater and the analysis of its adsorption kinetics.

2. Sodium alginate as biochar-alginate beads supporting material

To enhance the ammonium removal from wastewater, a combining system of sludge-based biochar, supporting material and activated sludge system was introduced in this research. The whole biochar-alginate beads system combined with surface physical adsorption, chemisorption, and further biological removal processes, which provided a recyclable and sustainable method for enhancing ammonium removal for wastewater treatment. Non-toxic polymers are widely agreed as the prefect supporting materials, in which polyvinyl alcohol (PVA) and sodium alginate (SA) are the two most commonly used support material (El-Naas, Mourad et al. 2013) to immobilize

bacteria (Kirdponpattara and Phisalaphong 2013), enzyme(Lin, Wang et al. 2013), yeast (Kirdponpattara and Phisalaphong 2013), antibodies (Monsalvo, Mohedano et al. 2011, Zielinska and Oleszczuk 2015)and to enhance their granule formation (Ania, Parra et al. 2002, Wenjie, Dunqiu et al. 2008) in wastewater (Yang, Pang et al. 2012, Wang, Ding et al. 2016) or solid waste treatment (Wang, Tian et al. 2016). PVA is widely used in textile printing and dyeing industry, but due to its varying solubility and long chain polymer structure, it is considered as a source of hardly remove containments (COD), which is a threat to the environment (Shaw, Carliell et al. 2002). Thus sodium alginate is considered as a safer, eco-friendlier and better support material in bacteria immobilization.

As one of the US Food and Drug Administration (FDA) -approved safe polymers (FDA 2016), sodium alginate is widely recognized as a natural non-toxic polysaccharide, which can be found in brown seaweeds. As sodium alginate is a readily processable three-dimensional scaffolding material, it has applied to a broad range of supporting matrix or delivery system for tissue repair and regeneration (Ania, Parra et al. 2002, Sun and Tan 2013). Due to the surface carboxylic functional groups, alginate beads are hydrophilic, which are excellent forming materials to hold a large amount of water and have the ability to stand high mechanical strength and high operation conditions (Przepiorski 2006). **Figure 1.1** below shows the two structures of alginate, which consists of natural carbohydrates and sodium salts. β -D-mannuronic acid (M) and α -L-guluronic acid (G) are the two compounds inside sodium alginate forming sequential 1,4-linkages with other materials (Rio, Faur-Brasquet et al. 2005) and are the basic components of the block structure of the polymer. When divalent cations (Ba^{2+} and Ca^{2+}) crosslink with guluronic acid, a chelated structure forming alginate gel, causing a three-dimensional network (Bajpai and Sharma 2004). The mechanism of ionic interaction of Ca^{2+} with carboxyl groups and the junction structures,

which is called “egg-box” junctions were shown in **Figure 1.2**. By using this mechanism, sodium alginate is selected for biochar-alginate beads formation and bacteria immobilization.

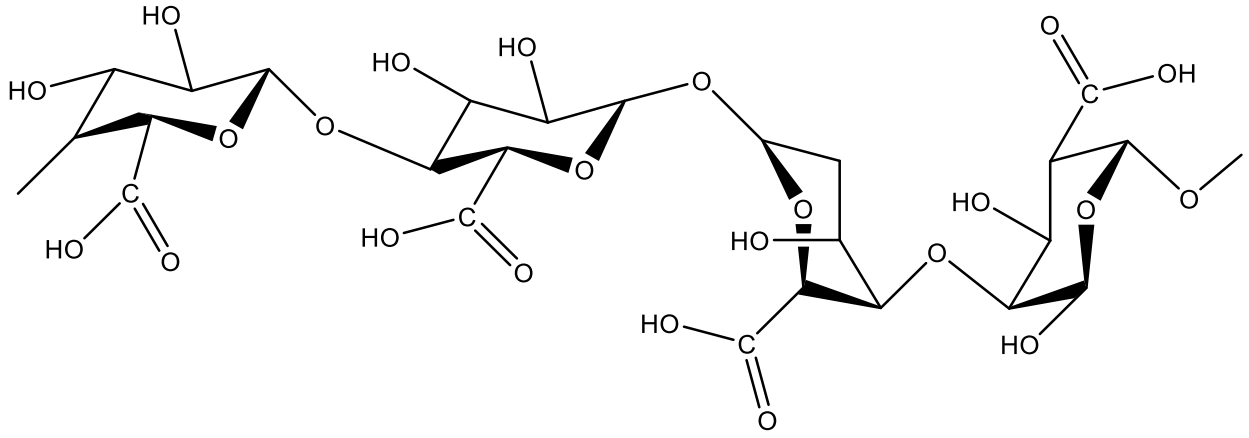

Figure 1.4 the 1,4-linkages of β -D-mannuronic acid (M) and α -L-guluronic acid (G)

For the researches of wastewater treatment processes, there are more papers focusing on the separate functions of two kinds of support materials, biochar, and sodium alginate (Silva, Manso et al. 2008, Li, Liu et al. 2010, Salisu, Sanagi et al. 2016). What’s more, the organic removal (Sandeman, Gun'ko et al. 2011) and heavy metals treatment (Zhang, Li et al. 2010, Hui, Zhang et al. 2015) in the wastewater were paid more attention, but combining support material and biochar (adsorbent) together with bacterial immobilization to removal inorganic containments from wastewater like ammonium were less noticed.

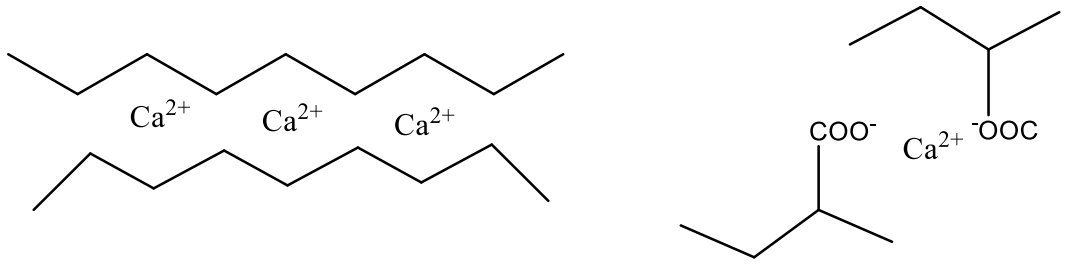

Figure 1.5 The “egg-box” structure and the Ca2+ interaction with COO- forming the alginate gel.

The characteristics of biochar-alginate beads were determined by following experiments, dyes adsorption tests, SEM, FTIR etc. Aside from, dye compounds may cause health problems when intake by human and animals, as an important parameter of mass transfer, blue dye adsorption, methyl blue, was tested in the following section as a crucial parameter of mass transfer (Poncelet 2001). The high methyl blue adsorption capacity indicates that biochar-alginate beads are able to transfer substances from aqueous into biochar-alginate beads. Through SEM, well-defined structures of sodium-alginate carbon beads were illustrated (Rocher, Siaugue et al. 2008). FTIR results showed that carboxyl and hydroxyl were the identical functional groups for biochar-alginate beads (Kumar, Tamilarasan et al. 2013). Other reaches reported that biochar and alginate have their own preference adsorbates. The carbonized biochar inside the combination of sodium alginate-carbon beads plays the role of the toxic organics adsorption and the alginate matrix takes the heavy metals away from the wastewater (Park, Kim et al. 2007). This paper also pointed out that activated carbon and alginate beads may be an alternative way of reverse osmosis conventional water purifier system(Park, Kim et al. 2007).

The method improvement of bacteria immobilized in different gels was discussed by Holmstrom et al. (Holmstrom, Steinberg et al. 2000). Different bacteria have been applied to biodegradation of various contaminants (de-Bashan and Bashan 2010). Immobilized isolated bacteria strain was used to degrade pollutions, like phenol (Wang, Tian et al. 2007), PAHs (Lee, Villaume et al. 2003) , Calcium (Fabre, Jezequel et al. 2003), COD and dyes (Kumar, Tamilarasan et al. 2013).

Aiming to enhance the overall ammonium removal capacity and evaluating the feasibility of bacteria embedded biochar-alginate beads, the beads were produced by combine sodium

alginate with activated sludge biochar and embedded with activated sludge from local wastewater treatment plant aerobic tank.

Chapter 2. Literature review: recent researches about using sludge-based biochar to wastewater treatment and their potential of bacteria carrier

1. Introduction

It is widely agreed that in the past decade environmental issues were getting more and more attentions. Sustainable and eco-friendly approaches are replacing traditional methods in a variety of industries. Waste sludge is the by-product of industrial activities, the residue of wastewater treatment, which can be considered as biosolids; however, based on Canadian federal acts and regulations, there is no clear definition of "sludge" or "biosolids" (2010). According to the report of Canadian Council of Ministers of the Environment, Canadian wastewater treatment facilities produced more than 660,000 metric tons (2.5 million wet tons) of dry stabilized biosolids annually (2012). The most common sludge is from wastewater treatment plants and wastes sludge treatment plants. Landfilling, incineration and agriculture are the most common approaches for treating waste sludge (Lu, Zhang et al. 2013). Sludge contains a large number of bacteria and pathogen, which is consider as biological and pathogenic hazards (Dumontet, Dinel et al. 1999). Waste sludge treatment is always combined with health threats and environmental concerns. The initial investment and operational cost for sludge treatment are hard for small cities to afford (2012).

1.1. Common sludge sources of biochar

The sources of sludge-based biochar are shown in **Table** 2.1. The most common sources are activated sludge from anaerobic digester; primary (physical treatment) settling tanks and secondary (biological treatment) settling tanks of BNR process in municipal wastewater treatment

plant; sewage sludge; industrial byproducts (like laundry industry, textile factory and paper mill); wastewater treatment plant sludge;1 and granular sludge from sequencing batch reactors.

Table 2.1 Sludge sources and different activation method

Raw material type	Pyrolysis condition			N_2 BET surface area (m^2/g)	Reference
	Temperature (℃)	Time (h)	Heating rate (℃/min)		
Anaerobic digester sludge	600℃	2 hours	10 ℃/min	161.2	(Inyang, Gao et al. 2012)
Anaerobic granular sludge	650℃	2 hours	15 ℃/min	741.14	(Shi, Zhang et al. 2014)
Sewage sludge from WWTP	from 700℃ (973K) to 900℃ (1173k)	40 to 80 mins	NA	185-395	(Zhai, Wei et al. 2004)
Anaerobically digested sugar beet tailings	600℃	2 hours	NA	23-297.5	(Yao, Lu et al. 2013)
No digestion treatment sludge	550℃	2 hours	10 ℃/min	24.73	(Lu, Zhang et al. 2012)
No digestion wastewater sludge from three different plants	300℃ 400℃ 500℃ 600℃	2 hours	10 ℃/min	NA	(Lu, Zhang et al. 2013)

1.2. The composition of different sludge

In order to treat and reuse sludge, it's necessary to know the composition of sludge. Besides, the constituents of sludge influence the characteristics of sludge-based biochar, which also affects by the application of wastewater treatment processes. The high organics content of sludge has been proven to enrich the carbon composition during pyrolysis process (Gascó, Blanco et al. 2005). The wet and untreated sludge contains protein, urea, grease, heavy metals, silica, and nitrogen (Izrail S. Turovskiy 2006). The main components of untreated digested sludge were evaluated and elaborated in **Table 2.2** (Eddy 2014). Secondary digester sludge has a higher

percentage of total dry solids, potash and nitrogen phosphorous concentration. On contrary, organic components, like protein, grease and fats, are more existing inside primary sludge. Heavy metals are important parameters for considering metal leaching when using biochar for wastewater treatment. Pyrolysis is the most common biochar treatment approach, which is significantly impacted by energy content (Hall 1995). Gasco et al.(Gasco, Blanco et al. 2005) defined humic substances, which can be categorized into two classes: fulvic acids with lower molecular weight and humic acid with higher molecular weight. The ratio of humic acid and fulvic acid is critically related to sludge types, as raw sludge represents higher ratio and digested sludge has a lower ratio, which is attributed to mineral fraction bonding (Mendez, Gasco et al. 2005).

Table 2.2 Typical chemical composition of untreated sludge and digested biosolids (Eddy 2014)

Item/sludge	Untreated primary		Digested primary		Untreated activated sludge
	Range	Typical	Range	Typical	Activated range
Total dry solids (TS), %	2.0-8.0	5.0	6.0-12.0	10.0	0.83-1.16
Volatile solids (% of TS)	60-80	65	30-60	40	59-88
Grease and fats (% of TS)					
Ether soluble	6-30	—	5-20	18	—
Ether extract	7-35	—	—	—	5-12
Protein (% of TS)	20-30	25	15-20	18	32-41
Nitrogen (N, % of TS)	1.5-4	2.5	1.6-6.0	3.0	2.4-5.0
Phosphorous (P2O5, % of TS	0.8-2.8	1.6	1.5-4.0	2.5	2.8-11.0
Potash (K2O, % of TS)	0-1	0.4	0.0-3.0	1.0	0.5-0.7
Cellulose (% of TS)	8.0-15.0	10.0	8.0-15.0	10.0	—
Iron (not as sulfide)	2.0-4.0	2.5	3.0-8.0	4.0	—
Silica (SiO2, % of TS)	15.0-20.0	—	10.0-20.0	—	—
pH	5.0-8.0	6.0	6.5-7.5	7.0	6.5-8.0
Alkalinity (mg/l as CaCO3)	500-1500	600	2500-3500	—	580-1100
Organic acids (mg/l as Hac)	200-20000	500	100-600	300	1100-1700
Energy content	10000-12500	11000	4000-6000	3000	6.5-8.0

1.3. Sludge-based biochar

Sewage sludge and activated sludge were first used and patented by Kemmer et al and Nalco Chemical Company in 1971 (Frank N Kemmer 1971) as a kind of raw material producing adsorbent under 300℃ to 900℃ for a certain time. Almost among the same time, by 1973, Beeckmans tested the sewage sludge's production and possible utilities by using high heat to carbonize sludge (Beeckmans and Ng 1971). After then, pyrolysis under an inert atmosphere is well used by researchers for carbonization to activate biochar surface. Temperature range from 500℃ to 800℃ was considered helpful for eliminating non-carbon material from raw material through gaseous volatile products (Goyal, Rattan et al. 2001). After pyrolysis, biochar is having a high porosity and large surface area carbonaceous material, which is due to the decomposition of organics and gas emission (Bansal, Garg et al. 2009). Pre-treatment methods or following pyrolysis with different modification methods can increase the surface area, pore volume or selected functional groups of biochar (Ahmadpour and Do 1997, Jindarom, Meeyoo et al. 2007). The detail of activation will be shown in the next section.

2. Activation methods of sludge-based biochar

2.1. Pyrolysis method

The pyrolysis method is the most common activation approach, which will optimize the surface area by high temperature. **Table 2.1** shows the part of the sludge-based biochar literature, using pyrolysis method, and its corresponding sludge source, holding time, heat rate and BET surface area. The highest surface area was obtained by using anaerobic granular sludge as raw material with 741.14 m^2/g (Shi, Zhang et al. 2014). According to the Zhai's (Zhai, Wei et al. 2004) and Nagreev's (Bagreev, Bandosz et al. 2001, Bagreev, Bashkova et al. 2001) research results, surface area and pore volume will increase as the extension of pyrolysis temperature and holding

time. The decomposition of organics and volatility of organics also helped the pore structure formation (Wang, Tian et al. 2016). The water release by dihydroxylation of inorganics process is considered as another reason of curving rough surface (Bagreev, Bandosz et al. 2001). There are some disagreements on whether dry sludge or little moisture remaining will enhance the activation or not. Zhai et al. proposed that 5% moisture remaining helped sludge self-activation, on the other hand, other researches (Lu, Low et al. 1995, Jeyaseelan and Qing 1996) proved that pre-dried sludge had a positive effect on the surface area. Pyrolysis temperature and heating rate as two main factors played an important role in BET surface area. Different reports showed various optimal pyrolysis temperatures for maximized surface area. Shi et al (Shi, Zhang et al. 2014). reported that under 650℃ for two hours has highest surface area 741.14m^2/g; While, 400℃ as the optimum pyrolysis temperature was reported by Zhang et al; few research groups (Lu, Low et al. 1995, Jeyaseelan and Qing 1996, Zhai, Wei et al. 2004) found 850℃ produced the highest surface area. Others different pyrolysis temperature reported include, 750℃(Silva, Ronix et al. 2016), 1000℃ (Rio, Faur-Brasquet et al. 2004), 650℃ (Inguanzo, Menendez et al. 2001) and 950℃ (Bagreev, Bandosz et al. 2001, Bagreev, Bashkova et al. 2001). These variations are due to the variability in the composition of different raw sludge material and also the pretreatment methods. Further reasons like different heating rate and activation time may all cause those diversities. From **table 2.2**, the common heating rates vary from 5℃/min to 15℃/min, besides, other faster heating rates are also evaluated (Jeyaseelan and Qing 1996). The relation between heating rate and physical properties of biochar/ activated carbon was reported, and higher heating rate yielded a slightly increased surface area (Marcilla, Asensio et al. 1996). With high pyrolysis temperature over 900℃ and long activation time, side effects like solidification and shrinkage of the carbonaceous matrix, which causes lower surface area and narrowing pore volume (Jeyaseelan and Qing 1996, Chiang,

Chao et al. 2001, Inguanzo, Menendez et al. 2001). During the initial stage of the pyrolysis process, polysaccharides volatilization and bond water loss are in charge of forming the macropores and mesopores. For the second stage of the process, relatively large pores are formed due to intermediate softening raw material and bubbling (Lu, Low et al. 1995).

2.2. Chemical activations

The detail of different reagents, activation conditions and surface area characteristics are shown in the Table 2.3. Different reagents and their efficiencies are discussed below.

Table 2.3 Surface area and detail of biochar produced by chemical activation

Sludge type	Activation conditions				Post-treatment	BET surface area	Reference
	Reagent	Reagent: Sludge ratio (by mass)	Temperature (°C)	Time (h)			
ADS	$ZnCl_2$	10g: 25mL of 5M $ZnCl_2$	500	2	3M HCl	647.4	(Chen, Jeyaseelan et al. 2002)
ACF	KOH/NaOH	2:1 or 8:1	750	1	5M HCl	644-2225	(Maciá-Agulló, Moore et al. 2004)
DS	$ZnCl_2$ and H_2SO_4	5g: 7M	440-950	0.5-3	H_2O	297	(Lu and Lau 1996)
SS	H_3PO_4, H_2SO_4 $ZnCL_2$	100g: 250ml 3M H_2SO_4 or 3M H_2PO_4 or 5M $ZnCl_2$	650	1	1M NaOH	137-555	(Zhang, Nriagu et al. 2005)
AS	H_2SO_4	0.5-1.5:1	400-900	1-3	NA	350-375	(Rio, Faur-Brasquet et al. 2005)
BS	$ZnCl_2$ and H_2SO_4	2:1	550	2	HCl	144.47	(Yu and Zhong 2006)
ScS	$ZnCl_2$ and H_2SO_4	$ZnCl_2$ 1:1 and 0.5:1 H_2SO_4 1:1 and 2:1	500	0.5 or 1	H_2O	171	(Martin, Balaguer et al. 1996)

SS	$ZnCl_2$ and H_2SO_4	1:1	650	5	HCl	NA	(Rozada, Otero et al. 2007)
ScS	$ZnCl_2$	3:1	850	NA	H_2SO_4/HCl	420-501	(Zhai, Wei et al. 2004)
SS	KOH	1:1	850	1	H_3SO_4 H_2O	658	(Shen, Guo et al. 2006)
SS	KOH	3:1	700	0.5	HCl	1686	(Ros, Lillo-Rodenas et al. 2006)
SS	NaOH	3:1	700	0.5	HCl	1224	(Ros, Lillo-Rodenas et al. 2007)

ACF: activated carbon fibers DS: dewatered sludge SS sewage sludge BS: biochemical sludge ScS: Secondary sludge

2.2.1 Base activation

From the surface area results, it's obvious that base activation is the most effective approach. By using sewage sludge as raw material, Maciá-Agulló et al, Shen et al and Ros et al, got the surface area of 644m^2/g, 658 m^2/g, and 1686 m^2/g, respectively. A "two-stage" theory may explain the high surface area that the sludge was carbonized prior to its impregnation and subsequent activation with the base. This theory was first reported by Ioannidou and Zabaniotou (Ioannidou and Zabaniotou 2007) and widely accepted by other researchers for processing different raw material. Few reasons for using allkaline reagent were reported: acid reagent first react with surface oxygen functional groups to form pores, but on the contrary, bases like NaOH and KOH, first react with carbon atoms to develop porosity (Ahmadpour and Do 1997, Hsu and Teng 2000). The bond water will lose during carbonization process, which provides more chance for base to access the surface of biochar (Smith, Fowler et al. 2009). Different impregnation methods had impacts on the surface area were also reported (Ros, Lillo-Rodenas et al. 2006, Lillo-

Ródenas, Ros et al. 2008) that dry conditions like physical mixing observed higher surface area than wet methods. The compositions in the sludge based biochar influenced the surface area as well. Under the same conditions, biochar which has higher carbon content and lower ash content were observed with significantly higher surface area than others. However, using water wash to intentionally decrease the ash content did not help surface area increase, which leads to a guess that inorganic compounds in the biochar made negative contributions to surface area (Lillo-Ródenas, Ros et al. 2008). The mechanisms of this guess are not clear (Smith, Fowler et al. 2009).

2.2.2 Acid activation

From table 2.3, comparing to base activation and $ZnCl_2$, acid activation is less efficient as the highest surface area value was only 408 m^2/g, which was obtained by Zhang et al. (Zhang, Nriagu et al. 2005). Acid was proved that it can react and oxidize material surface, which helped the surface cave to increased surface area. An earlier report showed that acid activation was sufficient to activate raw material at low temperature, however, by the year 2002, acid with the raw material under lower temperature was tested and proven that only at higher temperature can raise the surface area significantly (Bagreev and Bandosz 2002).

2.2.3 $ZnCl_2$ activation

$ZnCl_2$ is a common and effective reagent for activating sludge. From table 2.3, 647.4m^2/g was the highest surface area value and observed by Lu et al. using 5M $ZnCl_2$ as a reagent(Lu, Low et al. 1995). The surface area of sludge based biochar is affected by ash content inside the raw material and the chemical reaction with the reagent. Other sludge sources with lower inorganic and ash content, like mill and paper sludge and mixtures of sewage sludge and biomass, can gain even higher surface area(Cho and Suzuki 1980, Tay, Chen et al. 2001, Sandi, Khalili et al. 2003), which indicate the characteristics and composition of sludge impact the BET surface area (Chen,

Jeyaseelan et al. 2002). Anaerobic digester sludge is well used as it has higher MLSS value, but for most of the BNR process of wastewater treatment plant, part of the primary solids (inorganics) runs into anaerobic digester as well, which cause its lower carbon contents. And this was also observed by Tay et al.(Tay, Chen et al. 2001) and Chiang (Chiang and You 1987) as the performance of anaerobic sludge based biochar was lower than other sludge sources. Thus, ash content in the sludge material is the fundament factor of getting the larger surface area. Another factor may due to the chemical reaction. It was reported (Ibarra, Moliner et al. 1991) that $ZnCl_2$ react with H_2S forming ZnS, during the raw material decomposition process, which increases the biochar surface as well.

The activation temperature, using $ZnCl_2$ as a reagent, is lower than using base and acid as activation reagent. It is reported that temperature around 500℃ to 650℃ (Cho and Suzuki 1980, Chiang and You 1987, Jeyaseelan and Qing 1996, Bagreev, Locke et al. 2001) was sufficient for sewage sludge biochar to form reasonable surface area, however, lower range temperatures may cause a decrease in surface area.

The mechanisms for $ZnCl_2$ promoting pore forming were evaluated. As a catalytic, $ZnCl_2$ helped aromatic amines to form carbon structures and developed pore structures. Also, $ZnCl_2$ is widely accepted as a kind of dehydrating reagent (Balci, Dogu et al. 1994) and as a tar formation suppressant during the high-temperature process, which protects mesoporous from blocking up (Balci, Dogu et al. 1994, Yue, Mangun et al. 2002).

3. Different kinds of adsorbate and the adsorption mechanisms

In this section, more detail of the biochar applications and potential technologies for improving their performance will be introduced and discussed based on published papers and

reports. Three categories of containments were focused on and well evaluated by using sludge-based sorbate to capture from wastewater system. They are elaborated as follows.

3.1. Heavy metals

The details of heavy metal captured by biochar in the literature are illustrated in table 2.4. Comparing activation methods, direct carbonization has been proven as the most effective and economical approach (Rio, Faur-Brasquet et al. 2005, Seredych and Bandosz 2006). Rio et al. reported pyrolysis under 800°C, and a 277 mg/g of Cu^{2+} was obtained. The Cu^{2+} removal mechanism was also detailed by (Inyang, Gao et al. 2012). The high content of Ca^{2+} impacted the process, because of the Ca^{2+} ion exchange with the Cu^{2+} from wastewater. Based on the ion exchange mechanism, lower pyrolysis temperature was reached with similar removal capacity. Other heavy metal cations involved similar processes (table 2.4). Seredych also pointed out that high pyrolysis temperature prevents its cation exchange due to the high degree of mineralization (Seredych and Bandosz 2006).

The surface area was found to have less impact on metal cation removal, which was observed that even lower surface area still uptake higher amount of metal cation (Pan, Lin et al. 2003, Seredych and Bandosz 2006). The pH of the solution is critical. Bouzid et al. (Bouzid, Elouear et al. 2008) found that when pH is lower than 2.5, the adsorption process will be prevented, which is because of increased competition from H^+ ion for the surface site(Smith, Fowler et al. 2009). The optimal pH condition is 7.3, but when pH is higher than 5.3, metal ions like Cu^{2+} and Mg^{2+}, started to hydrolyze and precipitate (Bouzid, Elouear et al. 2008).

The post-treatment found promoting the metal cation capacity. HNO_3 has effectively increased the capacity of Na^+, Ca^{2+} and Mg^{2+}. This may be due to the acid removing the soluble

exchange ion on the surface of the biochar, which was substituted with H^+ ions, thus boosting the char's capacity(Mendez and Gasco 2005).

From table 2.4, chemical activation was used to promote the capacity of sludge-based biochar. $ZnCl_2$, HNO_3, and H_2SO_4 are common chemical reagents. Zhat et al.(Zhai, Wei et al. 2004) produced sludge-based biochar by $ZnCl_2$ and H2SO4, which has 8 to 10 times higher capacity compared to commercial activated carbon. The mechanism is that chemical activation introduced high functional group content and high cation exchange capacity(Martin, Artola et al. 2002, Martin, Artola et al. 2003). In conclusion, for higher metal cation uptake, a suitable surface chemical, higher cation exchange capacity and acidic surface functional groups were needed (Yin, Aroua et al. 2007).

Table 2.4 Metal cation uptake by biochar

Sludge type	Activation condition			Post-treatment	BET surface	Target sorbate Uptake	Mechanism	Reference
	Reagent	Temperature (℃)	Time (h)					
NDS	NA	550	2	H_2O	24.73	Pb^{2+}:30.88mg/g	1.Metal exchange 2.Complexation with free surface functional groups	(Lu, Zhang et al. 2012)
ADS	NA	600	2	H_2O	161.2	Pb^{2+}:99% Cu^{2+}:98% Ni^{2+}:26% Cd^{2+}:57%	1.Surface electrostatic 2.Surface Precipitation	(Inyang, Gao et al. 2012)
DTS+Al	NA	300℃ 400℃ 500℃ 600℃	1 or 2 hours	NA	23.72 at 400℃	Pb^{2+} Cr^{5+}	1.Pb^{2+} sorption at pH 5 involves metal exchange coprecipitation. 2.Cr5+ sorption relies on low pH	(Zhang, Mao et al. 2013)
ADS	NA	300	1	NA	155.51	Cr^{5+}:89% As^{5+}:53%	Cr (IV) electrostatic interactions	(Agrafioti, Kalderis et al. 2014)
MS	NA	900	20mins	NA	67.603	Cr^{3+}:7 mg/g Cr^{5+}:20 mg/g	Form Cr(OH)3 to precipitate	(Chen, Zhou et al. 2015)

IS	$ZnCl_2$	700	2	H_2O	1196	V^{5+} :37.17 mg/g	Chemical interaction	(Dogan and Aydin 2014)
AS+P	NA	800	45 mins	HCl	123-426	Cd^{2+}:27% Cr^{2+}-:88% $Pb2^{+}$:90% Ni^{2+}: 2% Zn^{2+}:80% As^{5+}:65% Se^{6+} :56%	NA	(Fitzmorris, Lima et al. 2006)
MS	$ZnCl_2$	850	NA	HCl	NA	Cd^{2+}: 62%, Ni^{2+}: 65%	ion exchange	(Zhai, Wei et al. 2004)
ADS	$ZnCl_2$	650	0.5	HCl	472	Hg^{2+}:175.4mg/g Pb^{2+}:64.1mg/g Cu^{2+}:30.7mg/g Cr^{3+}:15.4mg/g	1.High BET surface area 2.Carboxyl and lactone groups of the surface	(Rozada, Otero et al. 2008)

3.2. Dyes and organics

Dyes are evaluated by researcher because it is the main pollutant in the wastewater. The details of different sludge based biochar and uptake of dyes were elaborated in table 2.5. Methylene blue as the most common adsorbate, was used for dye uptake capacity (Martin, Artola et al. 2002, Otero, Rozada et al. 2003, Dhaouadi and M'Henni 2008). Methylene blue has a relatively high molecular weight and long structure chain, which tends to be maximized on mesoporous adsorbents (Sing, Everett et al. 1985). It is widely accepted that high mesoporosity is the factor of high methylene blue uptake(Girgis, Yunis et al. 2002). By analysis, the components of the biochar and high ash content limited the mesoporosities formation, which is a hamper for methylene blue uptake (Rozada, Otero et al. 2005). Besides these factors, the surface area and activation method are also key parts of high dye capacity (Calvo, Otero et al. 2001). Biochar formed by carbonization, $ZnCl_2$ or H_2SO_4 had a high methylene blue uptake. The dye itself is the factor for preventing high uptake value. The difference between anionic and cationic dyes was revealed by Jindarom, using sludge-based biochar with different dyes(Jindarom, Meeyoo et al. 2007). According to their

results, cationic dyes has 5 times greater up taking value than anionic dyes, which was attributed to dye's anionic nature and the electrostatic repulsion with biochar surface. Other researchers also found that cationic dyes were adsorbed in greater quantities than anionic dyes (Seredych and Bandosz 2007).

Table 2.5 Dye and organics uptake by sludge-based biochar

Sludge type	Activation condition			Post-treatment	BET surface	Target sorbate Uptake	Mechanism	Reference
	Reagent	Temperature (°C)	Time (h)					
Anaerobic granular sludge	ZnCl2	650°C	2	HCL	741.14	Methylene blue: 90.91mg/g	1.Electrostatic interaction 2.Cation exchange 3.Surface complexation	(Shi, Zhang et al. 2014)
Anaerobic tank	None	800 °C	2	HCL	NA	Malachite Green: 388.65mg/g	1.Cation exchange 2.Surface complexation	(Zhang, Liu et al. 2016)
Sewage sludge / tea waste (ratio 1:1)	None	300	1	None	NA	Methylene blue: 8.79mg/g	1.Ion exchange 2.Surface complexation	(Fan, Tang et al. 2016)
Sludge type	Activation condition			Post-treatment	BET surface	Target sorbate Uptake	Mechanism	Reference
	Reagent	Temperature (°C)	Time (h)					
Industrial laundry sewage sludge	None	750°C 800°C 850°C	2	None	65-159	Remazol Brilliant Blue R: 33.5mg/g	Surface complexation	(Silva, Ronix et al. 2016)
Sewage is from sedimentation tank of a textile factory	KOH H_3PO_4	600	1	HCL		Dye wastewater COD:95%		(Chen, Wang et al. 2015)
Anaerobic digester sludge from WWTP	H_2SO_4	625	0.5	HCL	390	Methylene blue and saphranine	Acceptable surface area	(Rozada, Calvo et al. 2003)
The sewage sludge is from sewage	None	Microwave at 800W	4min	None	2.62	Rhodamine 6G:13.3mg/g		(Annadurai, Juang et al. 2003)

treatment plant								
Sewage sludge		950	0.5	NA	108	Acid Red: 63mg/g	Cation exchange	(Seredych and Bandosz 2007)
Corn Stalk and Sewage sludge	NA	600	1	NA	59	Acid Red 18: 30mg/L		(Li, Li et al. 2016)

3.3. Phenol and phenolic compounds

Table 2.6 shows the phenolic compounds adsorbed by sludge based biochar, the basic physical properties of the biochar and the mechanisms of phenolic compounds uptake. Comparing to other containments previously shown, the uptaken phenol was found to be relatively low, which can be connected to its small molecular size (Przepiorski 2006). High degree of microporosity and surface chemical bonding are the two main factors for phenol removal. As there was a high ash content in the biochar, a lower microporosity was associated with sludge based biochar compared to commercial activated carbon. However, it was reported that surface chemical bonding surmounts the limitations of micropore (Rio, Faur-Brasquet et al. 2005). Chemical activation like $ZnCl_2$ was proved to have an influence on surface chemistry, which enhanced the phenol and phenolic compounds removal (Tay, Chen et al. 2001, Ania, Parra et al. 2002). The mechanisms of phenol and phenolic compounds adsorption were not clear. Surface functional groups are proposed to have negative impacts on adsorption. Yin found that the increasing of acid functional groups limited phenol uptake, besides, carboxyl and hydroxyl groups would also inhibit adsorption process (Karanfil and Kilduff 1999, Dabrowski, Podkoscielny et al. 2005). Physisorption and surface polymerization were reported by Leng (Leng and Pinto 1997) as the main mechanisms for phenol uptake. Other factors like metal and presence of oxygen were also found as the necessary aspects of promoting phenol uptake processes (Grant and King 1990).

Table 2.6. Phenol and phenolic compounds uptake by sludge-based biochar

Sludge type	Activation condition			Post-treatment	BET surface	Micros pore volume (cm^3/g)	Phenol Uptake (mg/g)	Mechanism	Reference
	Reagent	Temperature (°C)	Time (h)						
Sewage sludge and tyres	none	650°C	0.5	none	60	0.04	9.8	1.mesopore structure 2.chemsirorption	(Rozada, Otero et al. 2005)
Secondary sludge	H_2SO_4	700	0.5	HCl	253	0.05	26.7	Pore structure	(Martin, Artola et al. 2002)
Activated sludge WWTP	none	500	1	HCl	215.6	0.13	39.41	Ion exchange	(Liu, Chen et al. 2015)
Paper mill sludge	$ZnCl_2$	700	1	HCl	316.3	0.44	15.04	Physical sorption	(Pirzadeh and Ghoreyshi 2014)
Aerobic granular sludge	KOH	750	4	water	1800	0.35	85%	1.Different functional groups 2.Physical sorption	(Monsalvo, Mohedano et al. 2011)
Activated dewatered raw sludge from WWTP	NONE	250-1000	1.2		1230 985 265	0.49 0.40 0.11	NA	Surface functional groups as an electron donor and aromatic ring as an electron acceptor.	(Mohamed, Andriantsif erana et al. 2011)
Sewage sludge	None	500 600 700	5	None	18.13-54.05	5.87-12.54	NA	1.ion-exchange 2. physical sorption surface area	(Zielinska and Oleszczuk 2015)

4. Conclusion

This chapter illustrated that sludge can be considered as feedstock for producing adsorbents, which provide an alternative and eco-friendly approach for waste sludge disposal and reuse. Based on the facts above, the characteristics of sludge-based biochar vary due to both raw material sources and the activation methods. Low ash contents were reported to have a positive impact on the surface area, which represented that pretreatments like sieving, water wash and HCl washing for reducing ash content in the raw material are necessary. However, high inorganic portion of biochar always has a high ion exchange capacity, which is critical for heavy metal and dye adsorption. The chemical activation, especially the base activation method, was found and proved to be the most effective way to achieve higher surface area. Other methods, like physical activation, may not produce high surface area biochar but can introduce different kinds of surface chemicals and functional groups, which can be used base on different wastewater components. The activation temperature and heat rate are critical to the surface properties. The excessive high temperature will cause tar formation, which blocks the surface area increase. Comparing to other containments, sludge based biochar has a relatively high capacity of phenol. The low microporosities of biochar is the main mechanism of capturing phenol and phenolic compounds. Similar to other containments, chemical activations resulted in low ash contents, producing more surface area and microporosities that can favor the adsorption processes.

Chapter 3. Influence of pyrolysis temperature on production of digested sludge biochars and its application of ammonium removal from municipal wastewater

1.Objectives

This chapter measures the ability of digested sludge pyrolyzed to biochar at different temperatures to adsorb ammonia from ammonium solution and from municipal wastewater, and evaluates the fit of the adsorption process to isothermal and kinetics models.

2. Materials and methods

2.1. Preparation of digested sludge

Anaerobic digester sludge was collected from a biological nutrient removal (BNR) Wastewater Treatment Plant in Alberta, Canada. The sludge sample was air-dried inside a fume hood at room temperature for one week, then further dried in an oven at 60 ˚C for 12 hours. The dried sludge sample was grounded (Homemax HL-2570), sieved through a 1 mm particle size griddle, and sealed in a container until use.

2.2. Biochar and solution preparation

Pyrolysis temperature gradients were performed at 50 ˚C temperature intervals from 350–550 ˚C in a muffle furnace. Dried, ground, digested sludge (30 grams) was weighed and placed in a crucible. The crucible was covered with aluminum foil and heated in a furnace in an N_2 flow of 25 mL/min. The furnace temperature was raised at a rate of 5 ˚C/min for 2 hours. Samples of heated sludge (biochar) were obtained from the crucible processed at 350, 400, 450, 500, and 550 °C,

cooled in the N_2 environment, weighed, washed with deionized water three times, oven-dried overnight, then sealed in containers and stored at room temperature until use. Biochar samples were labeled as BC 350, BC 400, BC 450, BC 500, and BC 550 according to the pyrolysis temperature.

The ability of the prepared biochar to adsorb ammonium was tested in synthetic ammonium solution and in raw municipal wastewater. The wastewater and ammonium solution were autoclaved at 121 ˚C, filtered (0.45 μm), and stored at 4 ˚C until use.

2.3. Analytical methods

Elements in the digested sludge and the biochar samples were characterized by an elemental analyzer (Flash 2000 HT Plus). Surface area and pore size distribution were determined based on Brunauer-Emmett-Teller (BET) theory by nitrogen (N_2) adsorption/desorption at 77 K using a surface and pore size distribution analyzer (Autosorb Quantachrome 1MP). Surface morphology changes in biochar samples under different treatment conditions were investigated with scanning electron microscopy (Philips / FEI (XL30)). Surface functional groups were recorded with a Fourier transform infrared (FTIR) spectrometer in the 560–400 cm^{-1} range (Spectrum 100, PerkinElmer Ltd, Bucks, UK). Biochar production yield percentages at different pyrolysis temperatures were determined with a laboratory scale balance (Denver Instrument. Co., USA) using weight differences between the dried digested sludge and the biochar after pyrolysis. Ammonium concentrations were measured with the Ammonium TNTplus vial test, HR (2-47 mg/L NH_3-N, HACH®, USA) and a benchtop spectrophotometer (DR 3900, HACH®, USA). Biochar pH was determined by adding biochar samples to fresh distilled water with a ratio of 1:5, mixing

the samples using a bench top shaker for 30 min at a speed of 110 rpm/min, and measuring the pH of the supernatant using a pH meter (EXTECH EC500).

2.4. Potentiometric titrations of BC450

BC450 (4 g/L) was grounded and suspended in 50 mL nano-pure water, and the mixture was purged with N_2 for 30 minutes to remove CO_2. To test the reversibility of biochar proton binding, biochar samples were titrated with 0.1 M NaOH from pH 3 to pH 10 followed by reverse titration with 0.1 M HCl from pH 10 to pH 3 using a Mettler Toledo T50 titrator. The titrator ran dynamically with a 0.5 µM minimum dose and a 0.15 mL maximum dose. Titration data were modelled using Fiteql 4 (Herbelin, 1999) to determine the acidity constant and the site concentrations for three-site models. A nonelectrostatic surface complexation modeling (NEM) approach was used to fit titration data using the charge balance equation,

$$[C_a\text{-}C_b] = [-Q] + [H^+] + [OH^-], \quad (1)$$

where C_a and C_b are the concentrations of acid and base, respectively, [-Q] is the negative excess charge, $[H^+]$ is the concentration of protons, and $[OH^-]$ is the concentration of hydroxyl ions.

2.5. Ammonium adsorption on biochar samples

Ammonium adsorption on BC 350, BC 400, BC 450, BC 500, and BC 550 was measured to determine the impact of pyrolysis temperature on biochar ammonium adsorption capacity. Adsorption experiments were carried out in triplicate. Biochar (2.0 g) was added to 200 mL ammonium solution (45 mg/L NH_4-N) in a 500 mL Erlenmeyer flask and shaken in a shaker at 100 rpm/min for a defined contact time at room temperature, then filtered through a 0.22 um pore size filter. The ammonium residual was analyzed using an ammonium test vial based on the method 10205 HR TNTplus 832 (HACH, Canada). The ammonium removal percentage and the amount

of ammonium adsorbed on different biochar samples were calculated based on the difference between initial and final residual concentrations of aqueous ammonium, as described in equations (2) and (3). In equation (2) the ammonium removal percentage is expressed as

$$\text{Ammonium removal percentage}(\%) = \frac{(C_0 - C_t)}{C_0} \times 100\%\,, \tag{2}$$

where C_0 is the initial ammonium concentration (mg/L) in the solution, C_t is the ammonium concentration at time t, and

$$Q_t = \frac{V(C_0 - C_t)}{W}, \tag{3}$$

where Q_t is the amount of ammonium adsorbed per unit weight of biochar (mg/g) at time t. V is the volume (L) of the ammonium solution, and W is the mass (g) of the adsorbent (Eddy, 2014).

2.6. The effect of the solution initial pH and adsorbate concentration

HCL and NaOH were used to adjust the ammonium solution pHs to 2, 4, 6, 8, and 10. Biochar (2.0 g) was mixed in 200 mL of 45 mg/L NH_4-N solution in a 500 mL Erlenmeyer flask in each pH conditions to determine the effect of pH on biochar ammonium adsorption. The stability constant for ammonium adsorption to BC450 under various pH was determined using least-squares optimization built in Fiteql 4 (Herbelin, 1999). The NH_3-ligand stability constant is

$$K_{Ln-NH3} = \frac{[R-Ln-NH_3]}{[R-L_n^-]a_{NH3}}, \tag{4}$$

where the equilibrium constant, $K_{Ln\text{-}NH3}$, is expressed as log K_{Ln-NH3} for experiments. [R-Ln-NH_3] is the concentration of the NH_3-ligand organic complex, [R−L_n^-] is the concentration of ligands, and a_{NH3} is the activity of NH_3 in solution. The effect of the adsorbate concentration

(ammonium concentration 2, 4, 6, 8, 10, 20, 40, and 80 mg/L) was evaluated under a neutral pH solution condition and a fixed biochar mass.

2.7. Adsorption isotherm and adsorption kinetics models

The adsorption isotherm experiments were carried out by mixing 2 g of biochar sample with 200 mL synthetic ammonium solution of different initial ammonium concentrations (2, 4, 6, 8, 10, 20, 40, and 80 mg/L) under constant temperature of 20 ℃ in an incubator shaker at 100 rpm for 24 h.

All experiments were carried out in triplicate. The experimental data were fitted to Langmuir and Freundlich adsorption isotherm models.

Langmuir and Freundlich isotherms are developed in Eqs (8), (9), (10), and (11):

$$q_e = \frac{Q_m K_a C_e}{1+K_a C_e}, \tag{8}$$

Eq (8) can be transformed to a linear model:

$$\frac{1}{q_e} = \frac{1}{Q_m k_a c_e} + \frac{1}{Q_m}, \tag{9}$$

$$R_L = \frac{1}{1+K_a C_e}, \tag{10}$$

$$q_e = K_F C_e^{1/nF}, \tag{11}$$

where K_a is the Langmuir constant, R_L is the separation factor (Langmuir, 1918)., Q_m is the maximum adsorption capacity, and K_F and n_f are Freundlich constants (Freundlich, 1906).

Adsorption kinetics were used to describe the adsorption mechanism and the interaction between adsorbent and adsorbate. The Lagergren pseudo-first order model was introduced by Lagergren (Lagergren, 1898). Pseudo-second order model were first introduced to simulate the

adsorption of heavy metals from waters (Blanchard et al., 1984). The Lagergren pseudo-first order kinetics model is e xpressed in Equations (3) and (4):

$$\frac{dQ}{dt} = k_1(Q_e - Q_t) \tag{3}$$

Integration of Eq. (3) over the boundary conditions t = 0 to t = t and $Q_t = 0$ to $Q_t = Q_t$ yields Eq. (4) (Ho & McKay, 1999),

$$Q_t = Q_e(1 - \exp(-k_1 t)) \tag{4}$$

A pseudo-second order kinetics model to analyze ammonium adsorption is expressed as

$$\frac{\mathrm{dQ}}{\mathrm{dt}} = k_2(Q_e - Q_t)^2 \tag{5}$$

Integration of Eq (5) over the boundary conditions t = 0 to t = t and $Q_t = 0$ to $Q_t = Q_t$ affords

$$\frac{1}{Q_e - Q_t} = \frac{1}{Q_e} + k_2 t. \tag{6}$$

Eq (6) can be rearranged to Eq (7) to obtain a linear relation (Ho & McKay, 1999).

$$\frac{t}{Q_t} = \frac{1}{k_2 Q_e^2} + k_2 t \tag{7}$$

3. Results and discussion

3.1. Biochar yield and elemental analysis

Our results showed that the pyrolysis temperature strongly affected the biochar yield. As shown in Table 3.1, biochar yield was negatively correlated with the pyrolysis temperature. The biochar weight loss at 350 ℃ was 29.74%, which was 13% lower than the BC 550. The pH of biochar steadily increased as the pyrolysis temperature increased, which may be explained by the

volatilzation of organic acids and phenolic substances at higher temperature conditions (Shinogi & Kanri, 2003; Zhang & Wang, 2016).

Table 3.1 Physicochemical properties of raw material and biochars at different pyrolysis temperatures

	Raw	BC 350	BC 400	BC 450	BC 500	BC 550
Total nitrogen (w/w%)	5.85	3.11	2.71	2.60	2.36	2.07
Total carbon (w/w%)	34.85	22.02	19.37	18.60	17.66	15.74
Total oxygen (w/w%)	24.82	14.88	12.68	11.89	10.90	9.22
Total hydrogen (w/w%)	4.20	1.73	1.31	0.95	0.76	0.61
Total Carbon/ Total Nitrogen ratio	5.95	7.07	7.14	7.16	7.36	7.60
Yield (wt%)		70.26±2.2	64.36±3.6	61.29±3.6	58.41±2.8	57.22±3.0
pH		8.57	8.63	9.47	10.41	10.60

Analyses of the carbonized biochar indicated that the elemental concentrations in the biochar varied with the pyrolysis temperature (Table 3.1). Between 350 and 550 °C, the total nitrogen, total hydrogen and total oxygen content decreased as the temperature increased, which may be attrbitued to the loss of volatile nitrogen species and loss of NH_4-N and NO_3-N componds which tend to convert to more stable pyridine componds at higher temperature. This process decomposed acidic functional groups, causing an increase in the biochar pH. The tempertaure increase also led to the reduction in the carbon content, in agreement with previous studies (Yu & Zhong, 2006). An increase in the C/N ratio was observed with an increase in pyrolysis temperature, which indicates the conversion of orgainc substances to inorganic substance (Lu et al., 2013).

3.2. Optimal pyrolysis temperature and FTIR

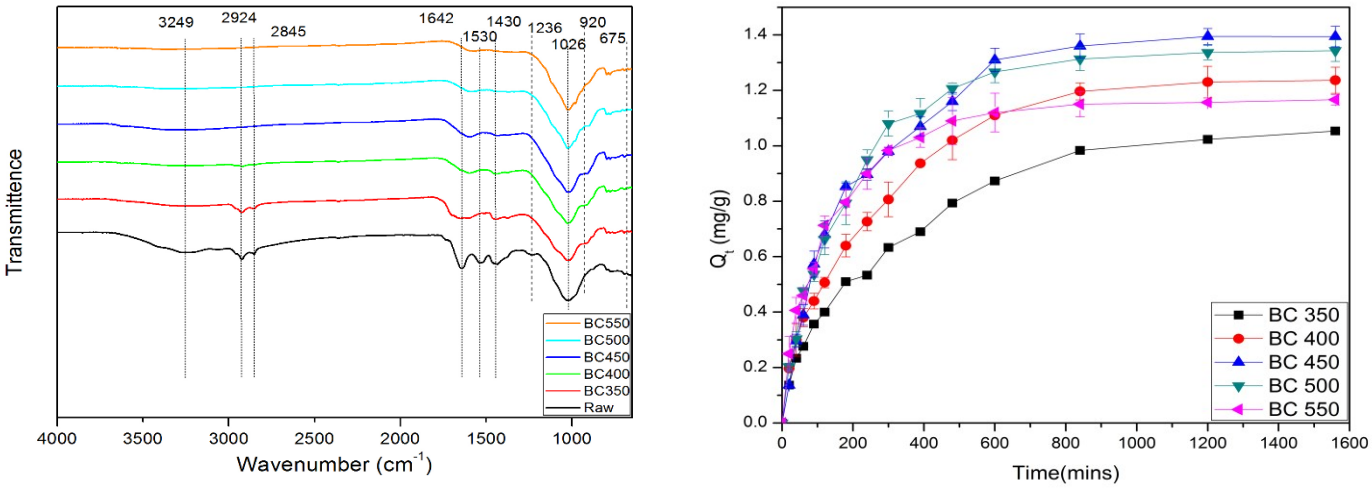

(a) (b)

Figure 6.1 (a) FTIR spectra of digested sludge and biochars treated at different pyrolysis temperatures, **(b)** Ammonia adsorption of biochars treated at different pyrolysis temperatures.

Figure 3.1 (a) shows surface functional group changes in anaerobic digested sludge and biochar samples detected by FTIR. After the pyrolysis temperature reached 400 ℃, only small differences in structure and functional groups were observed in biochar samples with further temperature increase. A strong adsorption band was observed from 3700 cm^{-1} to 3200 cm^{-1}, with a peak maximum at 3249 cm^{-1}, which was assigned to -OH stretching (Peng et al., 2016) and N-H in proteins. Asymmetric and symmetric stretching in CH_3 groups at 2924 cm^{-1} and 2845 cm^{-1} (Lin et al., 2012), respectively, were present in the sludge and BC350. Organic nitrogen in amines (1240 cm^{-1}) and amides (1530 cm^{-1}) were absent at temperatures higher than 350 ℃, and CH_3 groups were unstable at elevated temperatures. The intensity of -OH and $–CH_3$ decreased significantly from the sludge initially heated at 350 °C to the biochar at 400 °C. Thus, methyl groups (CH_3),

OH groups, and NH groups are weak functional groups (J. Jin et al., 2016). As the temperature increased, gas emission and thermal decomposition of functional groups caused the sludge to carbonize and pores to proliferate. On the other hand, aromatic rings (1642 cm^{-1}) and carboxylic acid (1430 cm^{-1}) were quite stable as the pyrolysis temperature increased, supporting crystallization. Clay and silica (1026 cm^{-1}) remained in the material. The small band at 920 cm^{-1}, apparent from 350 ℃ to 500 ℃, indicated the presence of polysaccharides or phosphodiesters (Gao et al., 2014). BC 550 showed a typical carbonized sludge with only a few peaks showed up.

Figure 3.1 (b) shows the removal of ammonium from synthetic ammonium solutions over time using biochar produced under different pyrolysis temperatures. Biochar with 450 ℃ pyrolysis temperature had the highest ammonium adsorption capacity. The maximum ammonium adsorption capacity for BC450 was 1.4 mg/g, similar to that of other raw material-based biochar (B. Wang et al., 2015). Due to the lack of carbonized and smaller surface areas, biochar pyrolyzed at lower temperatures (BC350, BC400) had relatively low ammonium adsorption capacities. The higher the pyrolysis temperature, the higher the surface area and pore size in the biochar samples were (Wannapeera et al., 2011). The loss of functional groups on the biochar surface might affect the ionic exchange during the adsorption process. BC450 and BC500 were the top two adsorbents. During the first 400 minutes, BC500 took a lead in the adsorption rate. The higher surface area in BC500, compared to surface area in BC450, could lead to a faster diffusion speed in BC 500.

3.3. Characteristics of biochar sample prepared at 450 °C

3.3.1. Scanning electron microscope (SEM) analysis and BET surface area analysis

BET surface areas of digested sludge and BC450 were 1.92 m^2/g and 20.86 m^2/g, respectively. Depolymerization and total char pore volume increase were observed from 0.364 cm^3/g to 0.664 cm^3/g , due to the high pyrolysis temperature (Lua et al., 2006).

As shown in the Figure 3.2, small holes and pits were observed in BC450. High pyrolysis temperature (450 °C) softened the sludge material and caused a release of organic volatile compounds and carbon crystallization (Zhong et al., 2016; Zielinska & Oleszczuk, 2016) These observations agree with BET surface analysis results. Pore size distribution at high temperature contributes to increases in surface area and pore volume (Huff & Lee, 2016; Purakayastha et al., 2015).

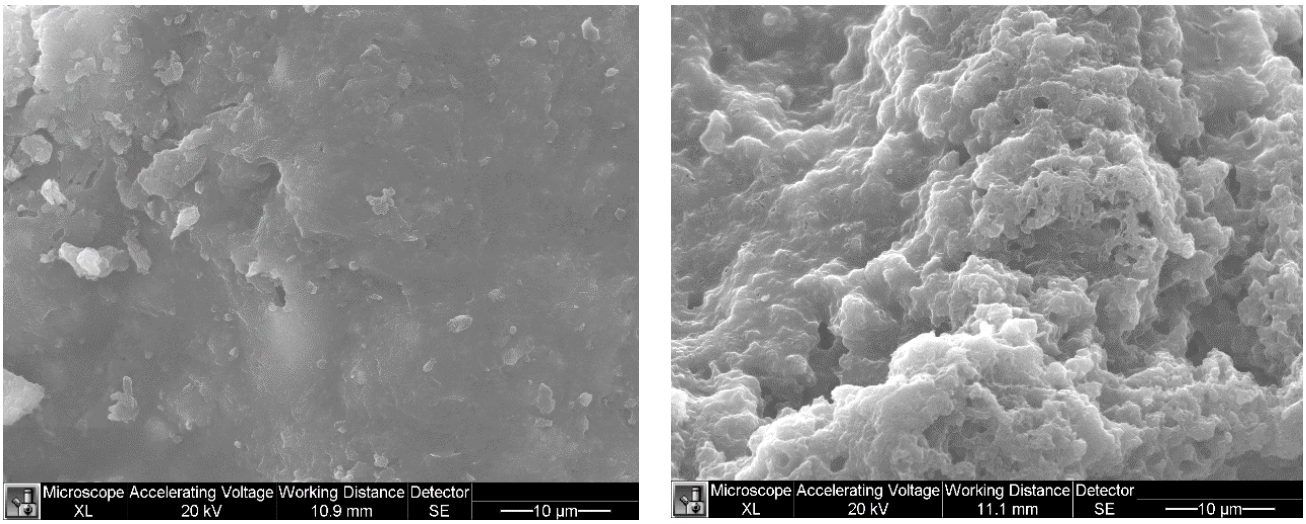

(a) (b)

Figure 3.2 SEM image of (a) digested sludge and (b) biochar sample BC450.

3.3.2. Potentiometric titration

Titrations with acid and base over the entire pH range indicated that biochar had significant

buffering capacity. Figure A1 and Table A1 show the excess charge per gram of BC450 biochar. There was no difference between titrations from acid to base and from base to acid, suggesting proton adsorption and desorption were reversible. The slope in Figure A1 represents the rate of ligand deportation and buffering capacity at any given point for a particular pH. The pronation model converged at three sites suggesting that three functional groups actively performed proton adsorption and desorption. The presence of biochar surface functional groups was verified by FTIR. The pKa and site concentrations of the functional groups are presented in Table A1. The pKa and the FTIR results indicate that BC450 had carboxylic, phenolic, and lactonic groups (Samrat Alam et al., 2016).

3.4. Effect of pH and initial ammonium concentration on ammonium adsorption by BC450.

Initial pH and initial ammonium concentration are important factors in biochar ammonium

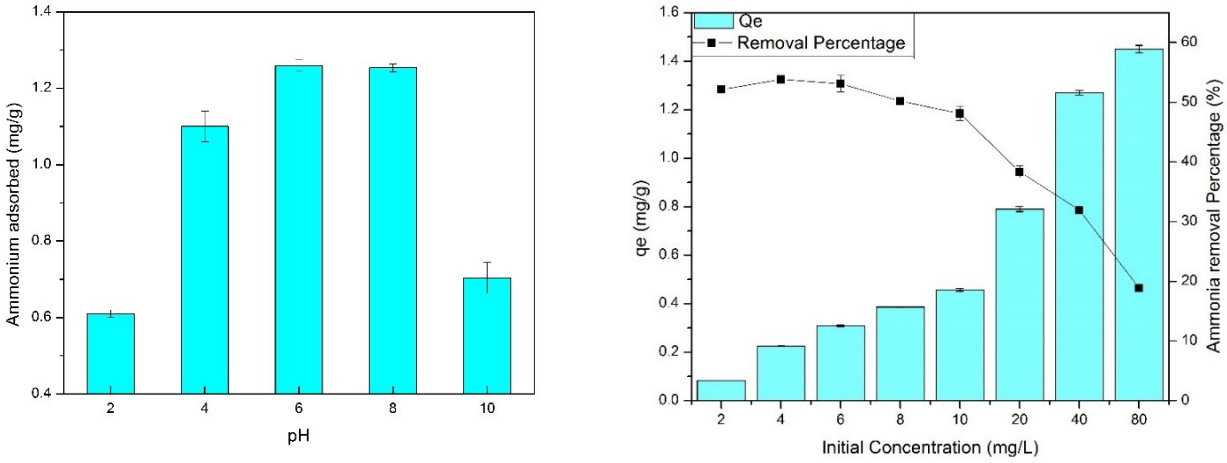

(a) (b)

Figure 3.3 Ammonium adsorption capacity of BC450 versus (a) initial pH (b) initial ammonium concentration.

adsorption. Figure 3.3(a) shows the amount of ammonium adsorbed on BC450 after 24 hours. The final amont of adsorbed ammonium increased as the initial pH increased from 2 to 6, resulting in

the optimal ammonium adsorption condition at pH 6. When pH was above 8, ammonium adsorption capacity reduced. The decline in the sorption capacity is due to the effects of pH on the state of ammonium (Vu et al., 2017). In the acidic condition, the ammonium removal capacity was low, which may be attributed to the strong competition between H^+ and NH_4^+ in the solution. Similar results have been reported by other researchers (Ismail & Hameed, 2014; Kizito et al., 2015; Moreno-Castilla, 2004; Vu et al., 2017). Ammonium adsorption data were modeled using Fiteql 4 to determine the stability constant of ammonium adsorption to BC450 ligands. Site concentrations of ammonium and pKas determined by potentiometric titration were used to calculate logKs of ammonium adsorption. Table A1 shows the stability constant of ammonium ligand reactions. Since the model showed best with first two pKas, it is assumed that ammonium mostly adsorbs to carboxyl and phenolic functional groups.

Using the same weight of biochar as adsorbent as previous adsorption analysis, Figure 3.3(b) shows the effect of the initial ammonium concentration on the biochar ammonium adsorption after 24 hours contact (adsorption equilibrium) and the ammonium removal percentage. The NH_4-N removal percentage reached a peak of 4 mg/L ammonium solution; after the peak value, the ammonium removal percentage reduced with an increase in the initial ammonium concentration. The removal percentage of adsorbate is a function of both the characteristics and concentration of the adsorbate (Eddy, 2014). The Q_e value increased as the initial ammonium concentration increased till it almost reached the maximum of the adsorption capacity. After the initial NH_4-N concentration reached 40 mg/L, the Q_e value increase became slower. When the initial NH_4-N concentration reached 80 mg/L, the Q_e value was almost the same as the theoretical adsorption capacity of biochar for ammonium, which was determined by developing its adsorption isotherm as described below.

3.5. Kinetics models and adsorption isotherm

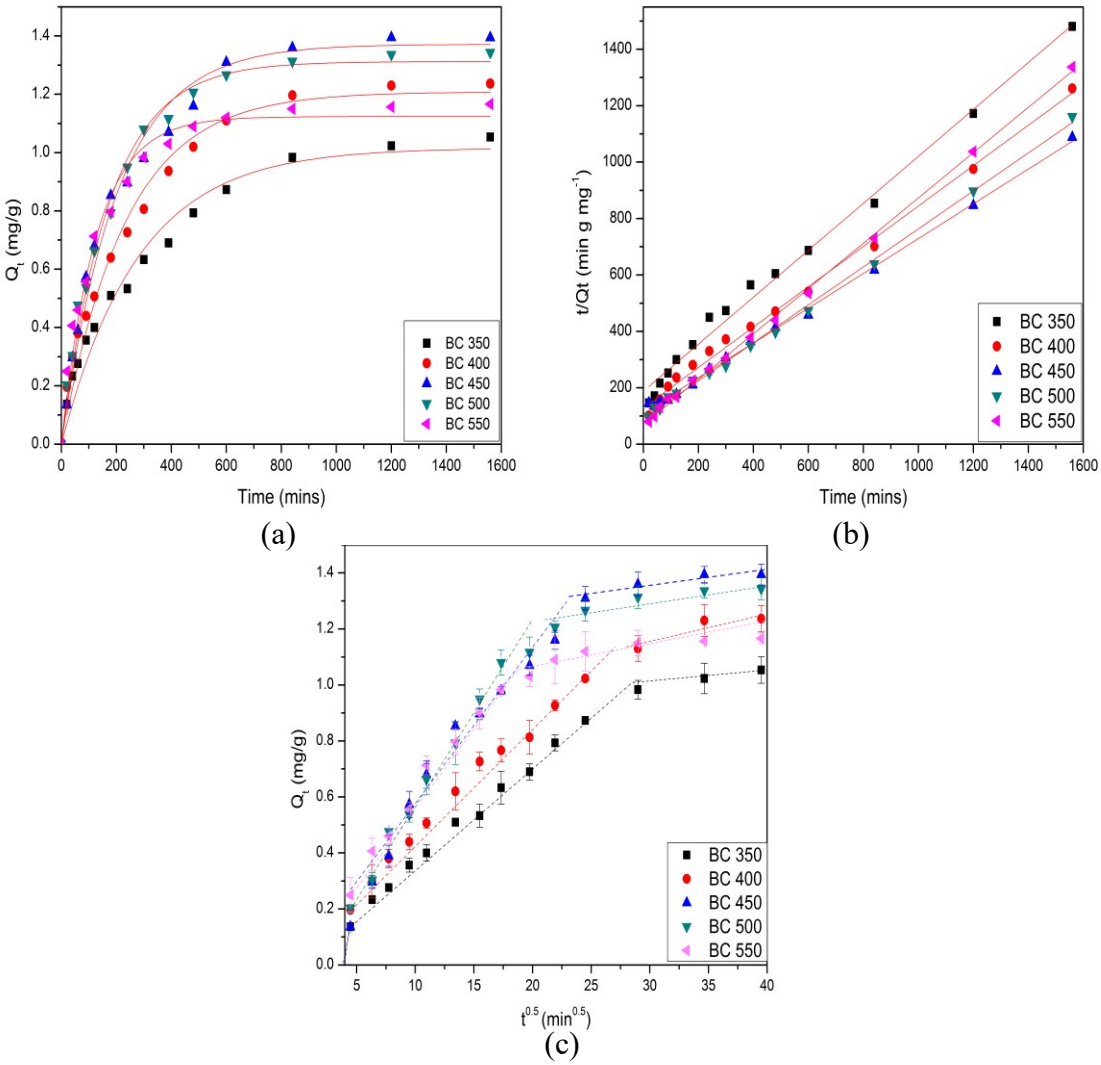

Figure 3.4 Biochar ammonium adsorption kinetics under (a) the Lagergren pseudo-first order model and (b) a pseudo-second order model, (c) intraparticle diffusion.

Isotherm models were used to define the relationship between adsorbate in liquid and solid (Hameed et al., 2008). The biochar ammonium adsorption capacity was evaluated using Langmuir and Freundlich adsorption isotherm models for single solute systems (Cazetta et al., 2011).

The Langmuir model is based on the assumption that adsorption occurs in a complete monolayer on a homogenous surface (Kannan & Sundaram, 2001). The separation factor (R_L) is the essential characteristic of the Langmuir isotherm (Weber & Chakravorti, 1974). According to (Ayoob et al., 2007), R_L represents the ratio of the remaining adsorption capacity over the total adsorption capacity. The adsorption in the system can be evaluated using the R_L value, if $0 < R_L < 1$, otherwise, the R_L value cannot be used to evaluate the adsorption (Cazetta et al., 2011). The higher R_L value of 0.995 of the Langmuir isotherm compared with the 0.950 in the Freudlich model indicates that the Langmuir isotherm fits the experimental situation better than the Freudlich model, and that the adsorption occurred largely in a monolayer on the biochar. An R_L value of less than 1 indicates that adsorption of ammonium from ammonium solution on the digested sludge biochar is favorable.

Kinetics models were used to clarify the reaction dynamics and reaction rates of ammonium adsorption to biochar. The experimental data were utilized to fit pseudo-first order and pseudo-second order models with the kinetics parameters shown in Table 3.2. According to the pseudo-second order model, the theoretical ammonium capacity of BC 450 is 1.52 mg/g, which is close to the experimental data 1.4 mg/g. The intra-particle diffusion plots in Figure 3.5 (c) show two-stages in biochar ammonium removal. The first stage corresponded to the adsorption process from 0–600 min ($t^{0.5}$ value: 0-25), which represented the intraparticle diffusion step and the rate-limiting step. In the second stage the adsorption reaches its equivalent point, that is, the adsorption and desorption speeds reached equivalence.

Table 3.2 Adsorption kinetics of biochar ammonium adsorption fitted to (a) a pseudo-first order model and (b) a pseudo-second order model

	Pseudo-first order			Pseudo-second order		
	Q_e（mg/g）	k_1 (min^{-1})	R^2	Q_e（mg/g）	k_2 (g/(mg·min))	R^2
BC 350	1.016	0.00357	0.9701	1.202	0.003674	0.9918
BC 400	1.208	0.00411	0.9694	1.397	0.003947	0.9953
BC450	1.372	0.00488	0.9828	1.521	0.003396	0.998
BC 500	1.312	0.00571	0.9913	1.486	0.005025	0.9981
BC 550	1.124	0.00791	0.9817	1.245	0.009111	0.9992

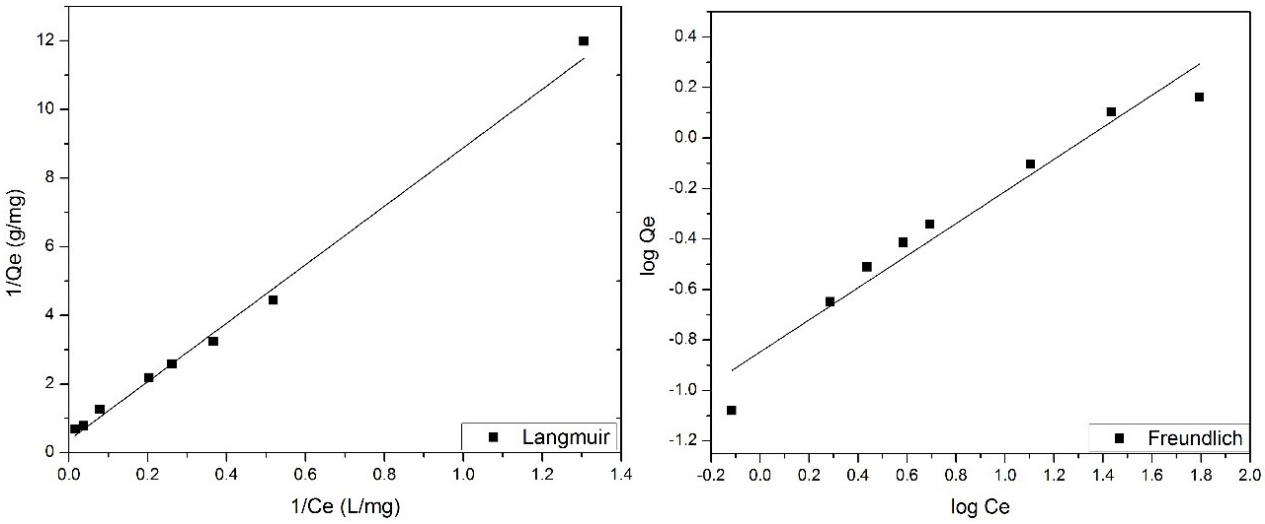

(a) (b)

Figure 3.5 Isotherm analyses of BC450 ammonia adsorption with (a) the Langmuir model and (b) the Freundlich model.

3.6. Digested sludge biochar applied to municipal wastewater

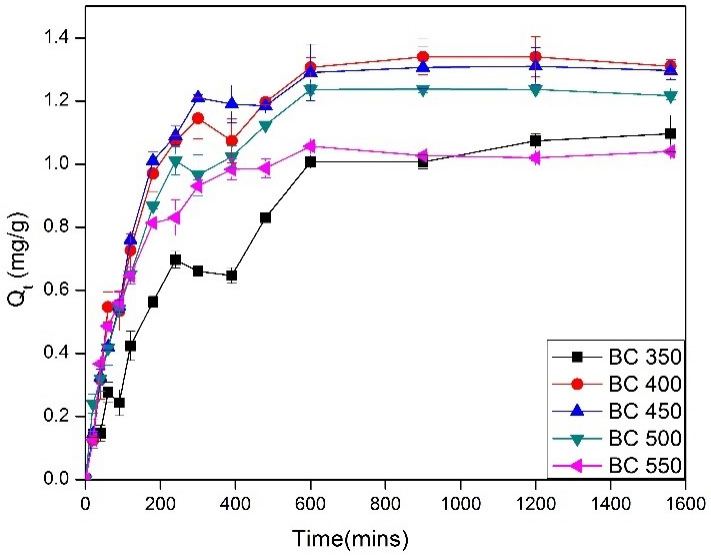

Figure 3.6 Removal of ammonium from municipal wastewater by biochars pyrolyzed at different temperatures.

Digested sludge was pyrolyzed at different temperatures and applied to remove ammonium from municipal wastewater obtained from the GBWWTP (Figure 3.6). Before applying the biochar to the municipal wastewater, the wastewater was sterilized to prevent interfere with ammonium adsorption. The biochar adsorption of ammonium from municipal wastewater (Figure 3.6) was similar to the biochar adsorption of ammonium from synthetic ammonium solution (Figure 3.1(b)), however, more fluctuations in adsorption were observed when testing the municipal wastewater. Most of the biochar samples presented sharp declines in ammonium adsorption in the first 400–600 min (Figure 3.1 (b)). Base on previous kinetics model and isotherm results, those declines may be attributed to limited pore transfer speed and untied bonded adsorptions (Eddy, 2014). The relatively large surface pore size and volume in digested sludge biochar allow the adsorption of high molecular organic particles, however, adsorption and desorption are ongoing processes and some pore positions can be taken by other wastewater contaminants (Xu et al., 2015), blocking the

entry of ammonium molecules and causing fluctuations in the ammonium adsorption curve. Similar results have been reported previously (Y. M. Wang et al., 2016). Most biochar samples had a lower ammonium adsorption capacity in the municipal wastewater than in the ammonium solution because of interference from compounds in the municipal wastewater (Y. M. Wang et al., 2016). Figure 3.1 (b) and Figure 3.6 indicate that 450 ℃ was the most effective pyrolysis temperature to implement digested sludge biochar ammonium adsorption, and future experiments with wastewater ammonium adsorption can benefit by observing this result.

4. Conclusions

In this study, digested sludge was pyrolyzed to improve its ammonium adsorption capacity. Biochar formed at 450 °C adsorbed ammonium from aqueous solution and municipal wastewater more efficiently than biochars pyrolyzed at lower and higher temperatures. The presence of carboxylic and phenolic functional groups in the biochar was confirmed by FTIR and Potentiometric titrations results. The initial ammonium concentration and pH of ammonium solution results showed that lower pH limited the capacity of digested sludge biochar and initial ammonium concentration has a positive relation with Q_e value. The biochar ammonium adsorption from municipal wastewater and aqueous ammonium solution fit a pseudo second-order kinetics model, which suggests that the process was controlled by chemisorption. Langmuir and Freundlich isotherms were used to analyze the relationship between adsorbate and adsorbent at the equilibrium point; the Langmuir model fit the experimental data better than the Freundlich model. We propose that digested sludge biochar can be used as an alternative w ay to remove ammonium from municipal wastewater.

Chapter 4. Enhanced ammonium removal through bacteria immobilized in sodium alginate biochar-alginate beads.

1.Objectives

This chapter focuses on (1) the optimal concentration of the sodium alginate to form alginate beads and to remove ammonium from aqueous system; (2) the best combination condition of sodium alginate and biochar to form biochar-alginate beads and enhance the ammonium removal from aqueous system; (3) the feasibility of sodium alginate and biochar as support materials to immobilize activated sludge (bacteria) for enhancing ammonium removal to achieve sustainable biological treatment process.

2. Methods and material

2.1. Adsorbent preparation

2.1.1 Biochar preparation

The dried digester sludge was pyrolyzed under 450℃ inside a muffle furnace which was constantly supplied with N_2 (>99.9%) at 25 ml min. Pyrolysis temperature was increased at a rate of 5℃/min from room temperature (20℃) up to 450℃ and was maintained at 450℃ for 2 hours. After the pyrolysis process, the biochar was cooled in the N_2 environment. The detail of the biochar produce has been elaborately described in pervious section (chapter 3 section 2.2).

2.1.2 Optimal concentration conditions of sodium alginate and biochar powder/ biochar-alginate beads preparation

The optimal concentration of sodium alginate required to form the sodium alginate beads was analyzed by combining sodium alginate and autoclaved deionized water, starting from 1% (w/w) up to 2.5% (w/w) with 0.5% (w/w) intervals. The optimal biochar concentration inside the

biochar-alginate beads was evaluated by measuring the adsorption capacity of the beads, which were produced by mixing selected alginate concentration from previous experiments, autoclaved deionized water and different biochar powder weight grades. In detail, selected mass of sodium alginate was mixed with 100mL of autoclaved deionized water, based on the previous experimental protocols, stirring for 1 hour. Subsequently, a centain weight of biochar was added into the sodium alginate mixture solution and stirred until the mixture became homogeneous. 1%, 3%, 5%, 7% and 9% (w/w) of biochar concentration were comined with sodium alginate and tested with ammonium solution to elvaluate biochar-alginate ammonium adsorption capacity (mg/g).

2.1.3. Bacteria Embedment

Based on the previous procedure for producing biochar-alginate beads, about 10ml of bacterial cell suspension was added to 90 ml of biochar-alginate solution, forming 100ml suspended mixture which was stirred for at least 2 hours. The resultant homogenous mixture was then dropped into 100ml of 2% (w/w) calcium chloride ($CaCl_2$) solution using a 12mL sterile syringe to form biochar-alginate droplets. The droplets were stirred inside calcium chlordie solution for at least 1 hour, forming bacteria embeded biochar-alginate beads. After that, the beads were rinsed with autoclaved deionized water several times to remove the excess unbonded calcium chloride. Then, the beads were placed inside the bio-safety fume hood for 2 hours until the residual water on the surface of the beads was dried up. Bacteria embeded biochar-alginate beads were directly used for subsequent experiments.

2.2. Mechanical property

The evaluation of mechanical property was based on the method described in (Zhang, Wu et al. 2007). 100 intact biochar-alginate beads were put into a 1L Erlenmeyer flask with 500mL deionized water, shaking at 120rpm min^{-1} for 72 hours. After the preset time, all the beads were

taken out and counted to determine the number of intact biochar-alginate beads. The percentage of intact biochar-alginate beads must over 95% before future analysis. The aim of this test was to evaluate the resistance of biochar-alginate beads under harsh operational conditions.

2.3. Mass transfer property

The mass transfer performance of biochar-alginate beads was evaluated by adsorption rate of methylene blue dye. A stock of high concentration methylene blue solution (1000 mg/L) was prepared in an amber colored volumetric flask. It was diluted to the 25mg/L by using deionized water. 2.0g of biochar-alginate beads were placed into an Erlenmeyer flask with 500mL of 25mg/L initial methylene blue dye with shaking for 24 hours at 120 rpm/min. The concentration of methylene blue in the flask was detected at 665 nm by spectrophotometer (DR 3900, HACH®, USA). After a series of preset time intervals, a relationship between the concentration of methylene blue dye and time was drawn. If the total removal percentage was over 95%, the biochar-alginate beads can be considered have good mass transfer performance.

2.4. Chemicals

Analytical grade ammonium chloride (NH_4Cl), sodium hydroxide (NaOH), calcium chloride ($CaCl_2$) and hydrochloride acid (HCl) were purchased from Fisher Chemical, Canada. The N_2 gas (>99.9%) was provided by Praxair Canada Inc, Edmonton, Canada. Sodium alginate (Alginic acid, sodium salt) was purchased from Acros Organics, Canada. The analytical grade methylene blue dye was purchased from Fisher scientific®, Canada..

2.5. Ammonium adsorption on the beads

To compare the ammonium adsorption kinetics, a series of samples: (1) bacteria, (2) biochar with bacteria, (3) sodium alginate beads, (4) sodium alginate beads embedded with

bacteria (5) biochar-sodium alginate beads and (6) biochar-sodium alginate bead embedded with bacteria were tested under ammonium solution condition. All the adsorption experiments were carried out in triplicates using 500mL Erlenmeyer flasks with 200mL of 45mg/L NH_4-N solution under the room temperature. The ammonium removal was determined by adding the same unit of each sample into the NH_4-N solution at time 0, shaking together at 100rpm min^{-1}. After a series of preset contact time, all the samples were filtered through 0.22um pore size filter. The residual ammonium was analyzed by following Salicylate method (Hach 2016). The ammonium removal percentage and the amount of ammonium adsorbed on different biochar were calculated by the difference between initial and final residual concentration of aqueous ammonium, which is described by following equations:

$$\text{Ammonium removal percentage (\%)} = \frac{(C_0 - C_t)}{C_0} \times 100\% \quad (1)$$

where, C_0 is the initial ammonium concentration in the solution (mg L^{-1}). C_e means at equilibrium point the ammonium concentration in the solution (mg L^{-1}).

$$Q_e = \frac{V(C_0 - C_t)}{W} \quad (2)$$

where, Q_e is at equilibrium point, the amount of ammonium adsorbed by per unit weight of biochar (mg/g). V is the volume of the ammonium solution (L). And, W is the mass of the adsorbent (g).

3. Results and discussion

3.1. The physical characteristics of biochar-alginate beads

The average diameter for biochar-alginate beads and sodium alginate beads are 4.3±0.3 mm and 3.2±0.2 mm, respectively. Small diameter beads are difficult to make and limit the mass transfer rate, which will reduce the contamination removal performance (Poncelet 2001). The ratio of the sodium concentration is critical for the biochar-alginate beads. According to experimental results, sodium alginate concentrations between 1% (w/w) to 2.5%(w/w) are able to form spherical shape biochar-alginate beads, which is consistent with other researchers (Buthe, Hartmeier et al. 2004, Lee, Ravindra et al. 2013). Fig 4.1 shows the digital photos of sodium alginate beads and biochar-alginate beads under conditions of wet (a, e), dry (b, f), 150×maginifation (e, g) and 1500×maginifaction (d, h).

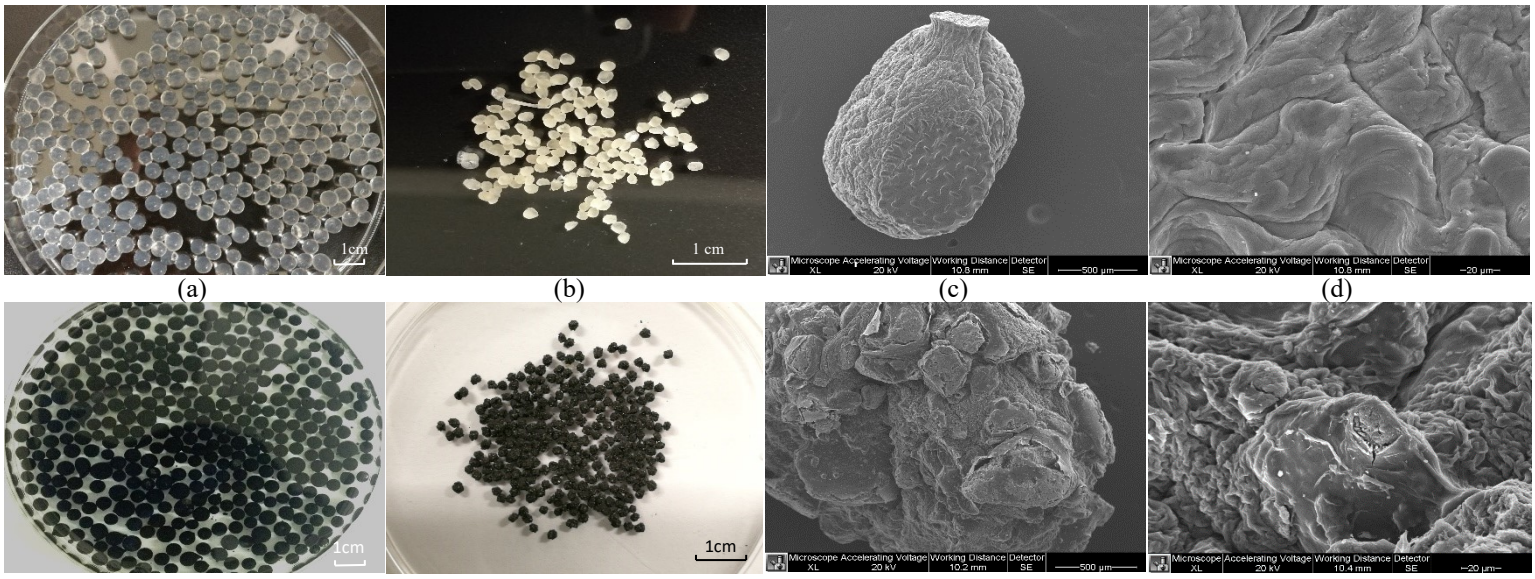

(a) (b) (c) (d)

(e) (f) (g) (h)

Figure 4.1 Digital photos of sodium alginate beads (a, b, c, d) and biochar-alginate beads (e, f, g, h)

Wet biochar-alginate beads and sodium alginate beads samples were found to be flexible and spherical in shape. Both dry biochar-alginate beads and dry sodium alginate beads shrink down to 1/10 of their regular size, which is because the sodium alginate's hydrophilic surface makes it

an excellent material for high water retention (Sun and Tan 2013). Figure 4.1 (c) shows a pineapple shaped sodium alginate bead with less rough surface compared to biochar-alginate beads in figure 4.1 (g). Under 1500× magnification, Figure 4.1 (d) clearly shows a lot of pleats exist on the sodium alginate beads surface. Besides, more rugged surface was observed in figure 4.1 (g), which enlarged the surface area.

The mass transfer was evaluated by using methyl blue adsorption results. Figure 4.2 shows that the system reaches an equilibrium at 6 hours with up to 99.2% of total methyl blue dye adsorbed by biochar-alginate beads. The ionic interaction of dye molecule and biochar-alginate beads surface function groups may be responsible for the adsorption processes (Jeon, Lei et al. 2008). The methyl blue removal percentage with time performance showed that Biochar-alginate beads have a very high mass transfer rate. High mass transfer percentage is the fundamental factor for bacteria immobilization as nutrients and containments can be easily transferred into the inside of biochar-alginate beads for the bacteria to utilize (Mater, Saucedo et al. 1999). Similar results were observed by other researches as well (Rocher, Siaugue et al. 2008, Eldin, Soliman et al. 2012, Liu, Wan et al. 2012).

A total number of 98 out of 100 biochar-alginate beads were intact after mechanical property tests, which proved that 1.5% (w/w) of sodium alginate combined with 2.5% (w/w) biochar powder can be used for future experiments.

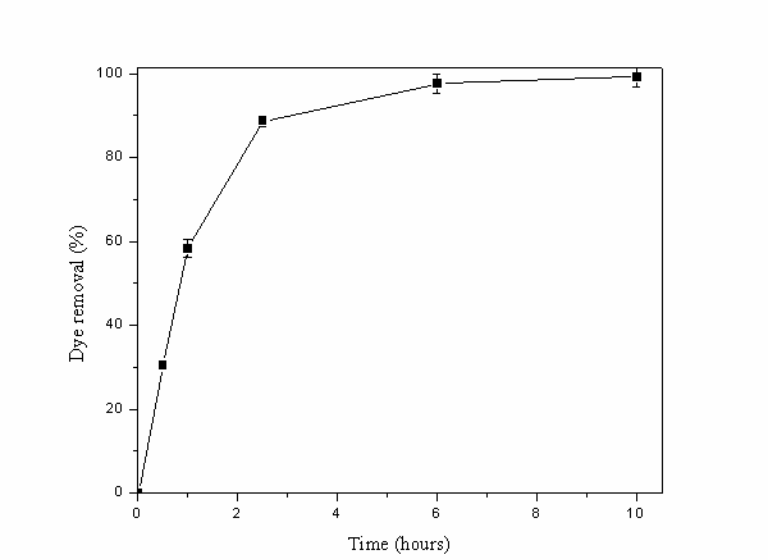

Figure 4.2 Methyl blue removal percentage of biochar alginate beads with contact time

3.2. The chemical characteristics

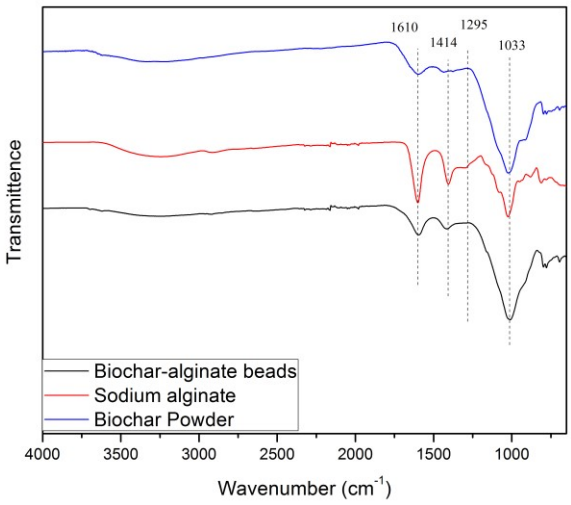

Figure 4.3 FTIR results of biochar-alginate beads, sodium alginate beads and biochar powder.

Surface functional groups are critical to ammonium adsorption capacity. Figure 4.3 shows the FTIR results of biochar-alginate beads, sodium alginate beads and biochar powder. The band at 3283 cm^{-1} for each of the samples is the -OH stretching, which represents the bonded hydroxyl groups. COO- (carboxylates) stretching existed for all three samples, however, the intensity of

carboxylate was enhanced by forming biochar-alginate beads, located in the band range from 1600-1680 cm^{-1} (Smidt, Bohm et al. 2011). The carboxylic acids are located at 1410-1430 cm^{-1}. There is also a shoulder band located at 1295 cm^{-1} on the sodium alginate sample indicating the appearance of C-O-C groups (Li, Du et al. 2013). C-O-C stretching represents the presence of polysaccharides. The strong peak located at 1026 cm^{-1} is attributed to silica for biochar and secondary hydroxyl group in the sodium alginate sample (-CH-OH in cyclic alcohols) (Li, Dai et al. 2008). Since the biochar was produced from secondary sludge of a municipal wastewater treatment plant, inorganic matter, such as stones and small rocks were present, which cannot be pyrolyzed under high temperature.

3.3 Results of batch adsorption

3.3.1 Results of optimizing sodium alginate concentration

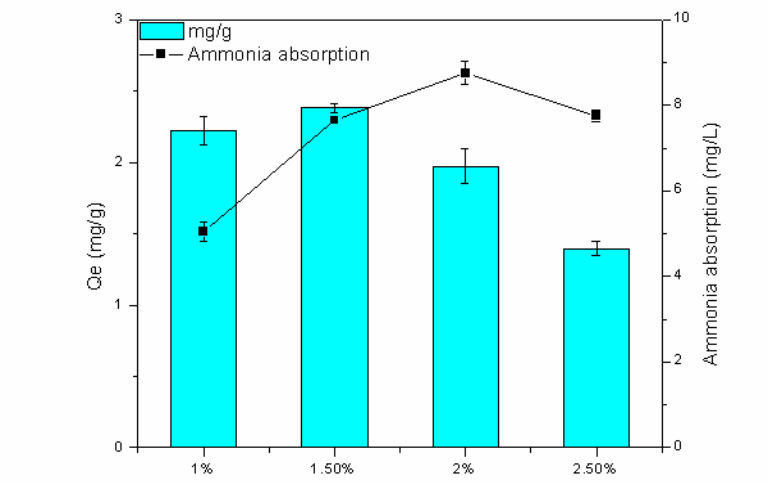

Figure 4.4 The effect of sodium alginate concentration and ammonium removal capacity, ammonium concentration removal.

Different concentration of sodium alginate beads adsorption capacity was evaluated under the same conditions to determine the optimal condition for supporting biochar and bacteria embedding. In Figure 4.4, shows the correlation between the ammonium adsorption capacity and

sodium alginate concentration. The line/scatter system shows the impact of sodium alginate concentration on the change in ammonium concentration. The adsorption capacity increased from 2.21 mg/g at sodium alginate beads with 1% (w/w) sodium alginate concentration till the peak value 2.38 mg/g at 1.5% of sodium alginate concentration, then dropped to 1.39 mg/g at 2.5% sodium alginate concentration of sodium alginate beads. The ammonium concentration removal (line and scatter) value increased till sodium alginate beads with 2% sodium alginate, where reached the highest ammonium removal concentration from aqueous among the all concentration conditions. The reason for this unequal optimal condition results is that sodium alginate beads with 2% sodium alginate concentration has a higher weight, thus providing more adsorbent for the removal process. (Davidovich-Pinhas and Bianco-Peled 2011, Yalcin, Apak et al. 2015) However, the total mass of 1.5% sodium alginate beads is lower than 2% sodium alginate beads, which causes the Q_e (mg/g) value (the capacity) of 1.5% to be higher than 2% sodium alginate beads. Thus, 1.5% sodium alginate was selected as optimal sodium alginate concentration for future experiments.

3.3.2 Results of optimizing biochar concentration

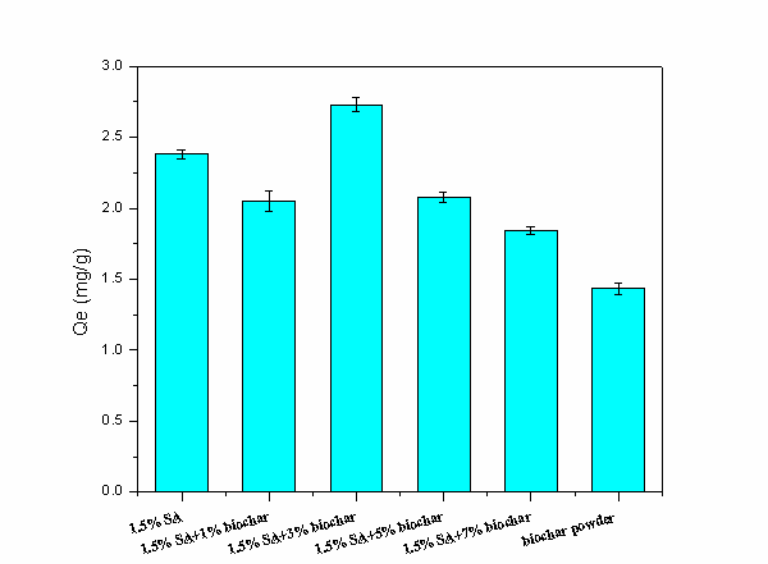

Figure 4.5 The effect of biochar powder concentration inside biochar-alginate beads on ammonium removal capacity (1.5% SA: sodium alginate beads with 1.5% (w/w) sodium alginate only; 1.5%+1% biochar: biochar-alginate beads contains 1.5% (w/w) sodium alginate and 1% (w/w) biochar powder; biochar powder: biochar only without sodium alginate. The other label followed the same pattern)

The results of biochar concentration inside biochar-alginate beads are shown in Figure 4.5. which were observed at the same initial conditions (ammonium concentration, pH, and temperature). By comparing the ammonium adsorption capacity of biochar powder and sodium alginate beads (1.5% SA), sodium alginate has an ammonium removal capacity of 2.38 mg/g, which is 60% higher than the 1.43 mg/g achieved from biochar powder. This is due to the sodium alginate beads having a higher surface functional group intensity and larger BET surface area (Smith, Fowler et al. 2009) than biochar powder. However, contradictory results were observed by other contaminants adsorption (Jodra and Mijangos 2003, Benhouria, Islam et al. 2015), due to different contaminants and adsorbents characteristics, such as molecular weight, surface charge,

and surface functional groups (Pawar and Edgar 2012), which can affect the adsorption results (Veglio, Esposito et al. 2002). There is a decrease in ammonium adsorption capacity of 1% biochar-alginate beads (1.5% SA+1% biochar). This may attribute to biochar taking part of the sodium alginate surface structural bonding site, which inhibited the sodium alginate from ammonium uptake. The ammonium removal capacity reached its peak at 3% biochar inside biochar-alginate beads and decrease to 1.43 mg/g as using biochar only. Thus, 3% of biochar and 1.5% sodium alginate were selected as the optimal biochar-alginate beads support material condition for future bacterial embed experiments.

3.4. Bacterial immobilization

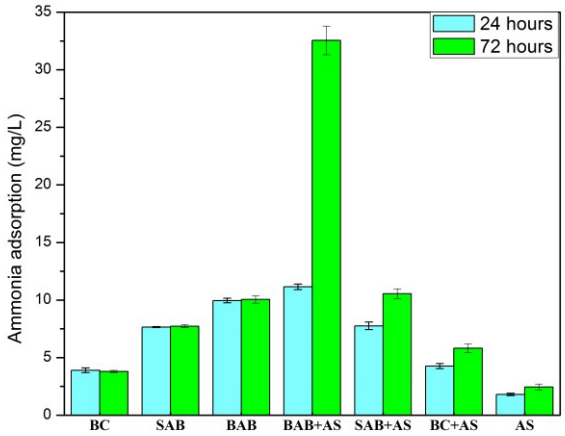

Figure 4.6 The ammonium adsorption of different adsorbents after 24 hours and 72 hours contact time. (BC: biochar powder; SAB: sodium alginate beads; BAB: biochar alginate beads; AS: activated sludge; BAB+AS: biochar beads embedded with activated sludge; SAB+AS: sodium alginate beads embedded with activated sludge; BC+AS: biochar powder with activated sludge)

The ammonium adsorption results were illustrated below in Figure 4.6. After a 24-hour adsorption test, the biochar-alginate beads (BAB) reached the equilibrium point, removing 10.65

mg/L ammonium. Due to the change from municipal wastewater of WWTP to ammonium solution, a lag phase might have occurred on the activated sludge (Ma, Peng et al. 2009). It was observed that only silently biological ammonium removal happened on the samples with activated sludge embedded (BAB+AS, SAB+AB, BC+AS). The ammonium concentration reduction of BAB+AS and AS were 11.15 mg/L and 1.8 mg/L, respectively. The ammonium reduction of sodium alginate beads (SAB) was at 7.65 mg/L, which was lower than biochar-alginate beads (BAB). The results of a 72-hour test showed a soar in the biochar-alginate beads with activate sludge embedded sample (SAB+AS), reaching 32.55 mg/L, indicating a change of ammonium removal mechanism might change (Villalobos, Acevedo et al. 2010). This accorded with the hypothesis that biochar-alginate beads with activate sludge embedded sample (SAB+AS) can produce a sustainable system with physical sorption, chemisorption and biological treatment. Also, a slight increase was observed in the activated sludge (AS) samples, showing that the biological treatment occurred on activated sludge samples. There were not any significant changes of the biochar-alginate beads (BAB) and sodium alginate beads (SAB) samples, as they already reached maximum ammonium adsorption and no further bacteria could uptake the ammonium on the surface of adsorbents. In addition, BCA+AS beads are pellet-like morphology (Zhang et al., 2008), which provide a suitable condition for bacteria growth (Grivel et al., 1999). And biochar can be considered as carbon source for bacteria to utilize, which promote the growth of autotrophic bacteria (Grivel et al., 1999).

4. Conclusion

The results of this study evaluated the feasibility of sodium alginate as a bacteria immobilization supporting material and an adsorbent to remove ammonium from wastewater. Based on physical characteristics, mass transfer and mechanical property results proved that sodium alginate is a suitable supporting material. The adsorption results showed that 1.5% (w/w) sodium alginate is the optimal concentration for both formatting alginate beads and remove ammonium from aqueous system. The best biochar concentration of sodium biochar-alginate beads combination is 3% (w/w), whose ammonium capacity is 2.74 mg/g. According to FTIR results, hydroxyl functional groups and carboxylic acids groups, which are crucial functional groups for ammonium adsorption were enhanced after sodium alginate beads were formatted. A lag phase was observed for all samples tested after 24 hours of reaction time. However, after 72 hours of reaction, biochar-alginate beads immobilized with bacteria taking up to 75 % of total ammonium, which approved that biochar-alginate beads can provide a suitable environment for bacteria to growth and able to transfer nutrients inside beads for bacteria utilization. Thus, biochar-alginate beads can enhance the overall ammonium removal by immobilizing with bacteria.

Chapter 5. Conclusions and future works

5.1. Conclusion

Base on the characteristics of activated sludge biochar; ammonium adsorption experiments results of both ammonium solution and municipal wastewater; characteristics of sodium alginate as supporting material; biochar sodium alginate beads ammonium capacity and activated sludge immobilize results, we draw following conclusions:

1) The optimal activated sludge pyrolysis temperature is 450℃, which increased the surface area. The SEM photos also showed dramatic surface changes after pyrolysis, which indicated more pore and hole structures were activated. The ammonium removal capacity is around 1.4 mg/g, which is comparable to biomass biochar results. pH is a main factor for affecting the ammonium removal. High pH (base condition) has a better ammonium removal percentage.
2) Two kinetic models of analyzing biochar powder, pseudo-first-order and pseudo-second-order model, were fitted to experimental data. Pseudo-second-order model has a better fitting of all the temperature biochar samples, which evaluated that the whole adsorption process is more inclined to chemisorption process. Further, intra-particle diffusion models evaluated a tree-step adsorption process, which proved the intraparticle diffusion step is the rate-limiting step. Comparing the isotherm model, Langmuir has a better fitting then Freundlich model, which provide the information that the adsorption only happened on the monolayer of adsorbent.
3) By using autoclaved municipal wastewater as a water source, a similar tendency was observed in the ammonium solution as a water source. Pyrolysis temperature 450℃ and 400℃ were all observed high ammonium removal capacity. Comparing to previous kinetics models, 450℃ has believed the optimal pyrolysis temperature on wastewater ammonium removal applications.
4) The optimal sodium alginate concentration of formatting beads and ammonium removal are 1.5% (w/w) and the best biochar concentration is 3% (w/w). The mass transfer and mechanical property test proved that biochar-alginate beads are able to provide transfer nutrients inside beads and can resist harsh operation condition. The overall ammonium

removal capacity is 2.74mg/g, which is almost twice the biochar powder capacity. The FTIR results illustrated that the hydroxyl functional groups and carboxylic acids group were enhanced after using sodium alginate as supporting material, which are two critical functional groups for ammonium removal from wastewater system.

5) A lag phase was observed after activated sludge embedded inside sodium alginate biochar-alginate beads. After 72 hours, a 75% of ammonium remove was reached, which indicated that the biochar-alginate beads can provide a suitable condition for bacteria growth.

5.2. Future works：

1) All the research results are based on lab-scale experiments. The data may vary when apply the biochar and biochar-alginate beads into upper-scale reactors.
2) Pilot-scale and full-scale evaluations are necessary before applying to industry. The number of beads to put into the reactor need to be evaluated.
3) Besides, beyond ammonium, other contaminants, like heavy metals and dyes, also need to be studied by using bacteria immobilized biochar-alginate beads.
4) The bacterial growth conditions and the microbial communities inside biochar-alginate beads requires further attention.
5) Other aspects, such as soil remediation, agriculture fertilizer and wetlands, may be interesting to focus on.
6) Using biochar-alginate beads as fixed bed media for wastewater treatment might be an interesting aspect.
7) Other format of biochar-alginate combinations (membrane, plastic carrier shape) can also be another research area.

Reference

(2010). A Review of the Current Canadian Legislative Framework for Wastewater Biosolids. C. C. o. M. o. t. Environment.

(2012). CANADA-WIDE APPROACH FOR THE MANAGEMENT OF WASTEWATER BIOSOLIDS C. C. o. M. o. t. Environment.

(2012). GUIDANCE DOCUMENT FOR THE BENEFICIAL USE OF MUNICIPAL BIOSOLIDS, MUNICIPAL SLUDGE AND TREATED SEPTAGE C. C. o. M. o. Envrioment.

Agrafioti, E., D. Kalderis and E. Diamadopoulos (2014). "Arsenic and chromium removal from water using biochars derived from rice husk, organic solid wastes and sewage sludge." Journal of Environmental Management **133**: 309-314.

Ahmadpour, A. and D. D. Do (1997). "The preparation of activated carbon from macadamia nutshell by chemical activation." Carbon **35**(12): 1723-1732.

Ahn, J. H., T. Kwan and K. Chandran (2011). "Comparison of Partial and Full Nitrification Processes Applied for Treating High-Strength Nitrogen Wastewaters: Microbial Ecology through Nitrous Oxide Production." Environmental Science & Technology **45**(7): 2734-2740.

Al-Wabel, M. I., A. Al-Omran, A. H. El-Naggar, M. Nadeem and A. R. A. Usman (2013). "Pyrolysis temperature induced changes in characteristics and chemical composition of biochar produced from conocarpus wastes." Bioresource Technology **131**: 374-379.

Ania, C. O., J. B. Parra and J. J. Pis (2002). "Effect of texture and surface chemistry on adsorptive capacities of activated carbons for phenolic compounds removal." Fuel Processing Technology **77**: 337-343.

Annadurai, G., R. S. Juang, P. S. Yen and D. J. Lee (2003). "Use of thermally treated waste biological sludge as dye absorbent." Advances in Environmental Research **7**(3): 739-744.

Ayoob, S., A. K. Gupta and P. B. Bhakat (2007). "Performance evaluation of modified calcined bauxite in the sorptive removal of arsenic(III) from aqueous environment." Colloids and Surfaces a-Physicochemical and Engineering Aspects **293**(1-3): 247-254.

Bagreev, A. and T. J. Bandosz (2002). "H2S adsorption/oxidation on materials obtained using sulfuric acid activation of sewage sludge-derived fertilizer." Journal of Colloid and Interface Science **252**(1): 188-194.

Bagreev, A., T. J. Bandosz and D. C. Locke (2001). "Pore structure and surface chemistry of adsorbents obtained by pyrolysis of sewage sludge-derived fertilizer." Carbon **39**(13): 1971-1979.

Bagreev, A., S. Bashkova, D. C. Locke and T. J. Bandosz (2001). "Sewage sludge-derived materials as efficient adsorbents for removal of hydrogen sulfide." Environmental Science & Technology **35**(7): 1537-1543.

Bagreev, A., D. C. Locke and T. J. Bandosz (2001). "H2S adsorption/oxidation on adsorbents obtained from pyrolysis of sewage-sludge-derived fertilizer using zinc chloride activation." Industrial & Engineering Chemistry Research **40**(16): 3502-3510.

Bajpai, S. K. and S. Sharma (2004). "Investigation of swelling/degradation behaviour of alginate beads crosslinked with Ca2+ and Ba2+ ions." Reactive & Functional Polymers **59**(2): 129-140.

Balci, S., T. Dogu and H. Yucel (1994). "CHARACTERIZATION OF ACTIVATED CARBON PRODUCED FROM ALMOND SHELL AND HAZELNUT SHELL." Journal of Chemical Technology and Biotechnology **60**(4): 419-426.

Bansal, M., U. Garg, D. Singh and V. K. Garg (2009). "Removal of Cr(VI) from aqueous solutions using pre-consumer processing agricultural waste: A case study of rice husk." Journal of Hazardous Materials **162**(1): 312-320.

Beeckmans, J. M. and P. C. Ng (1971). "PYROLYZED SEWAGE SLUDGE - ITS PRODUCTION AND POSSIBLE UTILITY." Environmental Science & Technology **5**(1): 69-+.

Benhouria, A., M. A. Islam, H. Zaghouane-Boudiaf, M. Boutahala and B. H. Hameed (2015). "Calcium alginate-bentonite-activated carbon composite beads as highly effective adsorbent for methylene blue." Chemical Engineering Journal **270**: 621-630.

Bouzid, J., Z. Elouear, M. Ksibi, M. Feki and A. Montiel (2008). "A study on removal characteristics of copper from aqueous solution by sewage sludge and pomace ashes." Journal of Hazardous Materials **152**(2): 838-845.

Bridle, T. R. and D. Pritchard (2004). Energy and nutrient recovery from sewage sludge via pyrolysis. Water Science and Technology. **50:** 169-175.

Bright, D. A. and N. Healey (2003). "Contaminant risks from biosolids land application: Contemporary organic contaminant levels in digested sewage sludge from five treatment plants in Greater Vancouver, British Columbia." Environmental Pollution **126**(1): 39-49.

Buthe, A., W. Hartmeier and A. B. Ansorge-Schumacher (2004). "Novel solvent-based method for preparation of alginate beads with improved roundness and predictable size." Journal of Microencapsulation **21**(8): 865-876.

Calvo, L. F., M. Otero, A. Moran and A. I. Garcia (2001). "Upgrading sewage sludges for adsorbent preparation by different treatments." Bioresource Technology **80**(2): 143-148.

Cao, X. D. and W. Harris (2010). "Properties of dairy-manure-derived biochar pertinent to its potential use in remediation." Bioresource Technology **101**(14): 5222-5228.

Cazetta, A. L., A. M. M. Vargas, E. M. Nogami, M. H. Kunita, M. R. Guilherme, A. C. Martins, T. L. Silva, J. C. G. Moraes and V. C. Almeida (2011). "NaOH-activated carbon of high surface

area produced from coconut shell: Kinetics and equilibrium studies from the methylene blue adsorption." Chemical Engineering Journal **174**(1): 117-125.

Chen, J. J., X. L. Wang, X. Y. Liu, J. G. Huang and Z. M. Xie (2015). "Removal of Dye Wastewater COD by Sludge Based Activated Carbon." Journal of Coastal Research: 1-3.

Chen, T., Z. Y. Zhou, S. Xu, H. T. Wang and W. J. Lu (2015). "Adsorption behavior comparison of trivalent and hexavalent chromium on biochar derived from municipal sludge." Bioresource Technology **190**: 388-394.

Chen, X., S. Jeyaseelan and N. Graham (2002). "Physical and chemical properties study of the activated carbon made from sewage sludge." Waste Management **22**(7): 755-760.

Chiang, H. L., C. G. Chao, C. Y. Chang, C. F. Wang and P. C. Chiang (2001). "Residue characteristics and pore development of petrochemical industry sludge pyrolysis." Water Research **35**(18): 4331-4338.

Chiang, P. C. and J. H. You (1987). "USE OF SEWAGE-SLUDGE FOR MANUFACTURING ADSORBENTS." Canadian Journal of Chemical Engineering **65**(6): 922-927.

Cho, B. R. and M. Suzuki (1980). "ACTIVATED CARBON BY PYROLYSIS OF SLUDGE FROM PULP-MILL WASTEWATER-TREATMENT." Journal of Chemical Engineering of Japan **13**(6): 463-467.

Dabrowski, A., P. Podkoscielny, Z. Hubicki and M. Barczak (2005). "Adsorption of phenolic compounds by activated carbon - a critical review." Chemosphere **58**(8): 1049-1070.

Davidovich-Pinhas, M. and H. Bianco-Peled (2011). "Physical and structural characteristics of acrylated poly(ethylene glycol)-alginate conjugates." Acta Biomaterialia **7**(7): 2817-2825.

de-Bashan, L. E. and Y. Bashan (2010). "Immobilized microalgae for removing pollutants: Review of practical aspects." Bioresource Technology **101**(6): 1611-1627.

Dhaouadi, H. and F. M'Henni (2008). "Textile mill effluent decolorization using crude dehydrated sewage sludge." Chemical Engineering Journal **138**(1-3): 111-119.

Dogan, V. and S. Aydin (2014). "Vanadium(V) Removal by Adsorption onto Activated Carbon Derived from Starch Industry Waste Sludge." Separation Science and Technology **49**(9): 1407-1415.

Dumontet, S., H. Dinel and S. B. Baloda (1999). "Pathogen reduction in sewage sludge by composting and other biological treatments: A review." Biological Agriculture & Horticulture **16**(4): 409-430.

Eddy, M. (2014). Wastewater engineering: treatment and resource recovery, Fifth edition, New York, NY: McGraw-Hill Education.

El-Naas, M. H., A. H. I. Mourad and R. Surkatti (2013). "Evaluation of the characteristics of polyvinyl alcohol (PVA) as matrices for the immobilization of Pseudomonas putida." International Biodeterioration & Biodegradation **85**: 413-420.

Eldin, M. S. M., E. A. Soliman, A. A. F. Elzatahry, M. R. Elaassar, M. F. Elkady, A. M. A. Rahman, M. E. Yossef and B. Y. Eweida (2012). "Preparation and characterization of imino diacetic acid functionalized alginate beads for removal of contaminants from waste water: I. methylene blue cationic dye model." Desalination and Water Treatment **40**(1-3): 15-23.

Fabre, B., K. Jezequel and T. Lebeau (2003). "Maximum uptakes of cadmium on free and immobilised bacteria and actinomycetes cells." Environmental Chemistry Letters **1**(2): 141-144.

Fan, S., J. Tang, Y. Wang, H. Li, H. Zhang, J. Tang, Z. Wang and X. Li (2016). "Biochar prepared from co-pyrolysis of municipal sewage sludge and tea waste for the adsorption of methylene blue from aqueous solutions: Kinetics, isotherm, thermodynamic and mechanism." Journal of Molecular Liquids **220**: 432-441.

Fan, Y., B. Wang, S. Yuan, X. Wu, J. Chen and L. Wang (2010). "Adsorptive removal of chloramphenicol from wastewater by NaOH modified bamboo charcoal." Bioresource Technology **101**(19): 7661-7664.

FDA, U. (2016). CFR - Code of Federal Regulations Title 21. U. S. F. a. F. Adminstration.

Fitzmorris, K. B., I. M. Lima, W. E. Marshall and R. S. Reimers (2006). "Anion and cation removal from solution using activated carbons from municipal sludge and poultry manure." Journal of Residuals Science & Technology **3**(3): 161-167.

Frank N Kemmer, R. D. M., Reid S Robertson (1971). Sewage treatment process. N. C. Co. USA.

Gao, N. B., J. J. Li, B. Y. Qi, A. M. Li, Y. Duan and Z. Wang (2014). "Thermal analysis and products distribution of dried sewage sludge pyrolysis." Journal of Analytical and Applied Pyrolysis **105**: 43-48.

Gasco, G., C. G. Blanco, F. Guerrero and A. M. M. Lazaro (2005). "The influence of organic matter on sewage sludge pyrolysis." Journal of Analytical and Applied Pyrolysis **74**(1-2): 413-420.

Gascó, G., C. G. Blanco, F. Guerrero and A. M. Méndez Lázaro (2005). "The influence of organic matter on sewage sludge pyrolysis." Journal of Analytical and Applied Pyrolysis **74**(1–2): 413-420.

Girgis, B. S., S. S. Yunis and A. M. Soliman (2002). "Characteristics of activated carbon from peanut hulls in relation to conditions of preparation." Materials Letters **57**(1): 164-172.

Goyal, M., V. K. Rattan, D. Aggarwal and R. C. Bansal (2001). "Removal of copper from aqueous solutions by adsorption on activated carbons." Colloids and Surfaces A: Physicochemical and Engineering Aspects **190**(3): 229-238.

Grant, T. M. and C. J. King (1990). "MECHANISM OF IRREVERSIBLE ADSORPTION OF PHENOLIC-COMPOUNDS BY ACTIVATED CARBONS." Industrial & Engineering Chemistry Research **29**(2): 264-271.

Hach (2016) "Nitrogen-Ammonium, Salicylate TNTplus Method 10205 (47 mg/L)."

Hall, J. E. (1995). "SEWAGE-SLUDGE PRODUCTION, TREATMENT AND DISPOSAL IN THE EUROPEAN UNION." Journal of the Chartered Institution of Water and Environmental Management **9**(4): 335-343.

Hameed, B. H., I. A. W. Tan and A. L. Ahmad (2008). "Adsorption isotherm, kinetic modeling and mechanism of 2,4,6-trichlorophenol on coconut husk-based activated carbon." Chemical Engineering Journal **144**(2): 235-244.

Herbelin, A. L. a. J. C. W. (1999). "FITEQL 4.0: A computer program for determination of chemical equilibrium constants from experimental data. Department of Chemistry." Oregon. Report 99-01.

Holmstrom, C., P. Steinberg, V. Christov, G. Christie and S. Kjelleberg (2000). "Bacteria immobilised in gels: Improved methodologies for antifouling and biocontrol applications." Biofouling **15**(1-3): 109-117.

Hospido, A., T. Moreira, M. Martín, M. Rigola and G. Feijoo (2005). "Environmental Evaluation of Different Treatment Processes for Sludge from Urban Wastewater Treatments: Anaerobic Digestion versus Thermal Processes (10 pp)." The International Journal of Life Cycle Assessment **10**(5): 336-345.

Hossain, M. K., V. Strezov, K. Y. Chan, A. Ziolkowski and P. F. Nelson (2011). "Influence of pyrolysis temperature on production and nutrient properties of wastewater sludge biochar." Journal of Environmental Management **92**(1): 223-228.

Hsu, L. Y. and I. Teng (2000). "Influence of different chemical reagents on the preparation of activated carbons from bituminous coal." Fuel Processing Technology **64**(1-3): 155-166.

Huff, M. D. and J. W. Lee (2016). "Biochar-surface oxygenation with hydrogen peroxide." Journal of Environmental Management **165**: 17-21.

Hui, B., Y. Zhang and L. Ye (2015). "Structure of PVA/gelatin hydrogel beads and adsorption mechanism for advanced Pb(II) removal." Journal of Industrial and Engineering Chemistry **21**: 868-876.

Ibarra, J. V., R. Moliner and J. M. Palacios (1991). "CATALYTIC EFFECTS OF ZINC-CHLORIDE IN THE PYROLYSIS OF SPANISH HIGH SULFUR COALS." Fuel **70**(6): 727-732.

Inguanzo, M., J. A. Menendez, E. Fuente and J. J. Pis (2001). "Reactivity of pyrolyzed sewage sludge in air and CO2." Journal of Analytical and Applied Pyrolysis **58**: 943-954.

Inyang, M., B. Gao, Y. Yao, Y. Xue, A. R. Zimmerman, P. Pullammanappallil and X. Cao (2012). "Removal of heavy metals from aqueous solution by biochars derived from anaerobically digested biomass." Bioresource Technology **110**: 50-56.

Ioannidou, O. and A. Zabaniotou (2007). "Agricultural residues as precursors for activated carbon production - A review." Renewable & Sustainable Energy Reviews **11**(9): 1966-2005.

Izrail S. Turovskiy, P. K. M. (2006). Wastewater Sludge Processing, Hoboken, N.J.: Wiley-Interscience.

Jeon, Y. S., J. Lei and J. H. Kim (2008). "Dye adsorption characteristics of alginate/polyaspartate hydrogels." Journal of Industrial and Engineering Chemistry **14**(6): 726-731.

Jeyaseelan, S. and L. G. Qing (1996). "Development of adsorbent/catalyst from municipal wastewater sludge." Water Science and Technology **34**(3-4): 499-505.

Jin, H., S. Capareda, Z. Chang, J. Gao, Y. Xu and J. Zhang (2014). "Biochar pyrolytically produced from municipal solid wastes for aqueous As(V) removal: Adsorption property and its improvement with KOH activation." Bioresource Technology **169**: 622-629.

Jin, J., Y. Li, J. Zhang, S. Wu, Y. Cao, P. Liang, J. Zhang, M. H. Wong, M. Wang, S. Shan and P. Christie (2016). "Influence of pyrolysis temperature on properties and environmental safety of heavy metals in biochars derived from municipal sewage sludge." Journal of Hazardous Materials **320**: 417-426.

Jindarom, C., V. Meeyoo, B. Kitiyanan, T. Rirksomboon and P. Rangsunvigit (2007). "Surface characterization and dye adsorptive capacities of char obtained from pyrolysis/gasification of sewage sludge." Chemical Engineering Journal **133**(1–3): 239-246.

Jindarom, C., V. Meeyoo, B. Kitiyanan, T. Rirksomboon and P. Rangsunvigit (2007). "Surface characterization and dye adsorptive capacities of char obtained from pyrolysis/gasification of sewage sludge." Chemical Engineering Journal **133**(1-3): 239-246.

Jodra, Y. and F. Mijangos (2003). "Phenol adsorption in immobilized activated carbon with alginate gels." Separation Science and Technology **38**(8): 1851-1867.

Kacan, E. (2016). "Optimum BET surface areas for activated carbon produced from textile sewage sludges and its application as dye removal." Journal of Environmental Management **166**: 116-123.

Kannan, N. and M. M. Sundaram (2001). "Kinetics and mechanism of removal of methylene blue by adsorption on various carbons - a comparative study." Dyes and Pigments **51**(1): 25-40.

Karanfil, T. and J. E. Kilduff (1999). "Role of granular activated carbon surface chemistry on the adsorption of organic compounds. 1. Priority pollutants." Environmental Science & Technology **33**(18): 3217-3224.

Kirdponpattara, S. and M. Phisalaphong (2013). "Bacterial cellulose-alginate composite sponge as a yeast cell carrier for ethanol production." Biochemical Engineering Journal **77**: 103-109.

Kumar, M., R. Tamilarasan and V. Sivakumar (2013). "Adsorption of Victoria blue by carbon/Ba/alginate beads: Kinetics, thermodynamics and isotherm studies." Carbohydrate Polymers **98**(1): 505-513.

Largitte, L. and R. Pasquier (2016). "A review of the kinetics adsorption models and their application to the adsorption of lead by an activated carbon." Chemical Engineering Research & Design **109**: 495-504.

Lee, B. B., P. Ravindra and E. S. Chan (2013). "Size and Shape of Calcium Alginate Beads Produced by Extrusion Dripping." Chemical Engineering & Technology **36**(10): 1627-1642.

Lee, H. J., J. Villaume, D. C. Cullen, B. C. Kim and M. B. Gu (2003). "Monitoring and classification of PAH toxicity using an immobilized bioluminescent bacteria." Biosensors & Bioelectronics **18**(5-6): 571-577.

Leng, C. C. and N. G. Pinto (1997). "Effects of surface properties of activated carbons on adsorption on behavior of selected aromatics." Carbon **35**(9): 1375-1385.

Li, L. and Y. Liu (2009). "Ammonia removal in electrochemical oxidation: Mechanism and pseudo-kinetics." Journal of Hazardous Materials **161**(2-3): 1010-1016.

Li, P., Y.-N. Dai, J.-P. Zhang, A.-Q. Wang and Q. Wei (2008). "Chitosan-Alginate Nanoparticles as a Novel Drug Delivery System for Nifedipine." International Journal of Biomedical Science : IJBS **4**(3): 221-228.

Li, Y. H., Q. J. Du, T. H. Liu, J. K. Sun, Y. H. Wang, S. L. Wu, Z. H. Wang, Y. Z. Xia and L. H. Xia (2013). "Methylene blue adsorption on graphene oxide/calcium alginate composites." Carbohydrate Polymers **95**(1): 501-507.

Li, Y. H., F. Q. Liu, B. Xia, Q. J. Du, P. Zhang, D. C. Wang, Z. H. Wang and Y. Z. Xia (2010). "Removal of copper from aqueous solution by carbon nanotube/calcium alginate composites." Journal of Hazardous Materials **177**(1-3): 876-880.

Li, Y. L., L. P. Li, X. J. Shi and Z. Wang (2016). "Preparation and analysis of activated carbon from sewage sludge and corn stalk." Advanced Powder Technology **27**(2): 684-691.

Lillo-Ródenas, M. A., A. Ros, E. Fuente, M. A. Montes-Morán, M. J. Martin and A. Linares-Solano (2008). "Further insights into the activation process of sewage sludge-based precursors by alkaline hydroxides." Chemical Engineering Journal **142**(2): 168-174.

Lin, Y., D. Wang and T. Wang (2012). "Ethanol production from pulp & paper sludge and monosodium glutamate waste liquor by simultaneous saccharification and fermentation in batch condition." Chemical Engineering Journal **191**: 31-37.

Lin, Y. H., S. H. Wang, M. H. Wu, T. M. Pan, C. S. Lai, J. D. Luo and C. C. Chiou (2013). "Integrating solid-state sensor and microfluidic devices for glucose, urea and creatinine detection based on enzyme-carrying alginate microbeads." Biosensors & Bioelectronics **43**: 328-335.

Liu, L., Y. Z. Wan, Y. D. Xie, R. Zhai, B. Zhang and J. D. Liu (2012). "The removal of dye from aqueous solution using alginate-halloysite nanotube beads." Chemical Engineering Journal **187**: 210-216.

Liu, Y. C., J. Chen, M. Y. Chen, B. Zhang, D. N. Wu and Q. X. Cheng (2015). "Adsorption characteristics and mechanism of sewage sludge-derived adsorbent for removing sulfonated methyl phenol resin in wastewater." Rsc Advances **5**(93): 76160-76169.

Liu, Y. X., D. S. Alessi, G. W. Owttrim, D. A. Petrash, A. M. Mloszewska, S. V. Lalonde, R. E. Martinez, Q. X. Zhou and K. O. Konhauser (2015). "Cell surface reactivity of Synechococcus sp

PCC 7002: Implications for metal sorption from seawater." Geochimica Et Cosmochimica Acta **169**: 30-44.

Lu, G. Q. and D. D. Lau (1996). "Characterisation of sewage sludge-derived adsorbents for H2S removal .2. Surface and pore structural evolution in chemical activation." Gas Separation & Purification **10**(2): 103-111.

Lu, G. Q., J. C. F. Low, C. Y. Liu and A. C. Lua (1995). "SURFACE-AREA DEVELOPMENT OF SEWAGE-SLUDGE DURING PYROLYSIS." Fuel **74**(3): 344-348.

Lu, H., W. Zhang, S. Wang, L. Zhuang, Y. Yang and R. Qiu (2013). "Characterization of sewage sludge-derived biochars from different feedstocks and pyrolysis temperatures." Journal of Analytical and Applied Pyrolysis **102**: 137-143.

Lu, H. L., W. H. Zhang, Y. X. Yang, X. F. Huang, S. Z. Wang and R. L. Qiu (2012). "Relative distribution of Pb2+ sorption mechanisms by sludge-derived biochar." Water Research **46**(3): 854-862.

Lua, A. C., F. Y. Lau and J. Guo (2006). "Influence of pyrolysis conditions on pore development of oil-palm-shell activated carbons." Journal of Analytical and Applied Pyrolysis **76**(1-2): 96-102.

Ma, Y., Y. Peng, S. Wang, Z. Yuan and X. Wang (2009). "Achieving nitrogen removal via nitrite in a pilot-scale continuous pre-denitrification plant." Water Research **43**(3): 563-572.

Maciá-Agulló, J. A., B. C. Moore, D. Cazorla-Amorós and A. Linares-Solano (2004). "Activation of coal tar pitch carbon fibres: Physical activation vs. chemical activation." Carbon **42**(7): 1367-1370.

Marcilla, A., M. Asensio and I. Martín-Gullón (1996). "Influence of the carbonization heating rate on the physical properties of activated carbons from a sub-bituminous coal." Carbon **34**(4): 449-456.

Martin, M. J., A. Artola, M. D. Balaguer and M. Rigola (2002). "Enhancement of the activated sludge process by activated carbon produced from surplus biological sludge." Biotechnology Letters **24**(3): 163-168.

Martin, M. J., A. Artola, M. D. Balaguer and M. Rigola (2002). "Towards waste minimisation in WWTP: activated carbon from biological sludge and its application in liquid phase adsorption." Journal of Chemical Technology and Biotechnology **77**(7): 825-833.

Martin, M. J., A. Artola, M. D. Balaguer and M. Rigola (2003). "Activated carbons developed from surplus sewage sludge for the removal of dyes from dilute aqueous solutions." Chemical Engineering Journal **94**(3): 231-239.

Martin, M. J., M. D. Balaguer and M. Rigola (1996). "Feasibility of activated carbon production from biological sludge by chemical activation with ZnCl2 and H2SO4." Environmental Technology **17**(6): 667-671.

Mater, D. D. G., J. E. N. Saucedo, N. Truffaut, J. N. Barbotin and D. Thomas (1999). "Conjugative plasmid transfer between Pseudomonas strains within alginate bead microcosms: Effect of the internal gel structure." Biotechnology and Bioengineering **65**(1): 34-43.

Mendez, A. and G. Gasco (2005). "Optimization of water desalination using carbon-based adsorbents." Desalination **183**(1-3): 249-255.

Mendez, A., G. Gasco, M. M. A. Freitas, G. Siebielec, T. Stuczynski and J. L. Figueiredo (2005). "Preparation of carbon-based adsorbents from pyrolysis and air activation of sewage sludges." Chemical Engineering Journal **108**(1-2): 169-177.

Mohamed, E. F., C. Andriantsiferana, A. M. Wilhelm and H. Delmas (2011). "Competitive adsorption of phenolic compounds from aqueous solution using sludge-based activated carbon." Environmental Technology **32**(12): 1325-1336.

Monsalvo, V., A. Mohedano and J. Rodriguez (2011). "Activated carbons from sewage sludge Application to aqueous-phase adsorption of 4-chlorophenol." Desalination **277**(1-3): 377-382.

Moreno-Castilla, C. (2004). "Adsorption of organic molecules from aqueous solutions on carbon materials." Carbon **42**(1): 83-94.

Otero, M., F. Rozada, L. F. Calvo, A. I. Garcia and A. Moran (2003). "Kinetic and equilibrium modelling of the methylene blue removal from solution by adsorbent materials produced from sewage sludges." Biochemical Engineering Journal **15**(1): 59-68.

Pan, S. C., C. C. Lin and D. H. Tseng (2003). "Reusing sewage sludge ash as adsorbent for copper removal from wastewater." Resources Conservation and Recycling **39**(1): 79-90.

Park, H. G., T. W. Kim, M. Y. Chae and I. K. Yoo (2007). "Activated carbon-containing alginate adsorbent for the simultaneous removal of heavy metals and toxic organics." Process Biochemistry **42**(10): 1371-1377.

Pawar, S. N. and K. J. Edgar (2012). "Alginate derivatization: A review of chemistry, properties and applications." Biomaterials **33**(11): 3279-3305.

Peng, C., Y. B. Zhai, Y. Zhu, B. B. Xu, T. F. Wang, C. T. Li and G. M. Zeng (2016). "Production of char from sewage sludge employing hydrothermal carbonization: Char properties, combustion behavior and thermal characteristics." Fuel **176**: 110-118.

Pirzadeh, K. and A. A. Ghoreyshi (2014). "Phenol removal from aqueous phase by adsorption on activated carbon prepared from paper mill sludge." Desalination and Water Treatment **52**(34-36): 6505-6518.

Poncelet, D. (2001). Production of alginate beads by emulsification/internal gelation. Bioartificial Organs Iii: Tissue Sourcing, Immunoisolation, and Clinical Trials. D. Hunkeler, A. Cherrington, A. Prokop and R. Rajotte. **944:** 74-82.

Przepiorski, J. (2006). "Enhanced adsorption of phenol from water by ammonia-treated activated carbon." Journal of Hazardous Materials **135**(1-3): 453-456.

Purakayastha, T. J., S. Kumari and H. Pathak (2015). "Characterisation, stability, and microbial effects of four biochars produced from crop residues." Geoderma **239**: 293-303.

Rio, S., C. Faur-Brasquet, L. Le Coq, P. Courcoux and P. Le Cloirec (2005). "Experimental design methodology for the preparation of carbonaceous sorbents from sewage sludge by chemical activation - application to air and water treatments." Chemosphere **58**(4): 423-437.

Rio, S., C. Faur-Brasquet, L. Le Coq and P. Le Cloirec (2005). "Structure characterization and adsorption properties of pyrolyzed sewage sludge." Environmental Science & Technology **39**(11): 4249-4257.

Rio, S., C. Faur-Brasquet, L. Le Coq, D. Lecomte and P. Le Cloirec (2004). "Preparation and characterization of activated carbon from sewage sludge: carbonization step." Water Science and Technology **49**(1): 139-146.

Rocher, V., J. M. Siaugue, V. Cabuil and A. Bee (2008). "Removal of organic dyes by magnetic alginate beads." Water Research **42**(4-5): 1290-1298.

Ros, A., M. A. Lillo-Rodenas, C. Canals-Batlle, E. Fuente, M. A. Montes-Moran, M. J. Martin and A. Linares-Solano (2007). "A new generation of sludge-based adsorbents for H2S abatement at room temperature." Environmental Science & Technology **41**(12): 4375-4381.

Ros, A., M. A. Lillo-Rodenas, E. Fuente, M. A. Montes-Moran, M. J. Martin and A. Linares-Solano (2006). "High surface area materials prepared from sewage sludge-based precursors." Chemosphere **65**(1): 132-140.

Rozada, F., L. F. Calvo, A. I. García, J. Martín-Villacorta and M. Otero (2003). "Dye adsorption by sewage sludge-based activated carbons in batch and fixed-bed systems." Bioresource Technology **87**(3): 221-230.

Rozada, F., M. Otero, A. I. García and A. Morán (2007). "Application in fixed-bed systems of adsorbents obtained from sewage sludge and discarded tyres." Dyes and Pigments **72**(1): 47-56.

Rozada, F., M. Otero, A. Moran and A. I. Garcia (2005). "Activated carbons from sewage sludge and discarded tyres: Production and optimization." Journal of Hazardous Materials **124**(1-3): 181-191.

Rozada, F., M. Otero, A. Morán and A. I. García (2008). "Adsorption of heavy metals onto sewage sludge-derived materials." Bioresource Technology **99**(14): 6332-6338.

Rozada, F., M. Otero, J. B. Parra, A. Moran and A. I. Garcia (2005). "Producing adsorbents from sewage sludge and discarded tyres - Characterization and utilization for the removal of pollutants from water." Chemical Engineering Journal **114**(1-3): 161-169.

Salisu, A., M. M. Sanagi, A. Abu Naim, W. A. W. Ibrahim and K. J. A. Karim (2016). "Removal of lead ions from aqueous solutions using sodium alginate-graft-poly(methyl methacrylate) beads." Desalination and Water Treatment **57**(33): 15353-15361.

Samrat Alam, M., M. Cossio, L. Robinson, X. Wang, J. P. L. Kenney, K. O. Konhauser, M. D. MacKenzie, Y. S. Ok and D. S. Alessi (2016). "Removal of organic acids from water using biochar and petroleum coke." Environmental Technology & Innovation **6**: 141-151.

Sandeman, S. R., V. M. Gun'ko, O. M. Bakalinska, C. A. Howell, Y. S. Zheng, M. T. Kartel, G. J. Phillips and S. V. Mikhalovsky (2011). "Adsorption of anionic and cationic dyes by activated carbons, PVA hydrogels, and PVA/AC composite." Journal of Colloid and Interface Science **358**(2): 582-592.

Sandi, G., N. R. Khalili, W. Q. Lu and J. Prakash (2003). "Electrochemical performance of carbon materials derived from paper mill sludge." Journal of Power Sources **119**: 34-38.

Seredych, M. and T. J. Bandosz (2006). "Removal of copper on composite sewage sludge/industrial sludge-based adsorbents: The role of surface chemistry." Journal of Colloid and Interface Science **302**(2): 379-388.

Seredych, M. and T. J. Bandosz (2007). "Removal of cationic and ionic dyes on industrial-municipal sludge based composite adsorbents." Industrial & Engineering Chemistry Research **46**(6): 1786-1793.

Shaw, C. B., C. M. Carliell and A. D. Wheatley (2002). "Anaerobic/aerobic treatment of coloured textile effluents using sequencing batch reactors." Water Research **36**(8): 1993-2001.

Shen, W. Z., Q. J. Guo, X. P. Yang, Y. H. Liu, Y. R. Song and J. Cheng (2006). "Adsorption of methylene blue in acoustic and magnetic fields by porous carbon derived from sewage sludge." Adsorption Science & Technology **24**(5): 433-437.

Shi, L., G. Zhang, D. Wei, T. Yan, X. Xue, S. Shi and Q. Wei (2014). "Preparation and utilization of anaerobic granular sludge-based biochar for the adsorption of methylene blue from aqueous solutions." Journal of Molecular Liquids **198**: 334-340.

Shi, L., G. Zhang, D. Wei, T. Yan, X. D. Xue, S. S. Shi and Q. Wei (2014). "Preparation and utilization of anaerobic granular sludge-based biochar for the adsorption of methylene blue from aqueous solutions." Journal of Molecular Liquids **198**: 334-340.

Shinogi, Y. and Y. Kanri (2003). "Pyrolysis of plant, animal and human waste: physical and chemical characterization of the pyrolytic products." Bioresource Technology **90**(3): 241-247.

Silva, R. M. P., J. P. H. Manso, J. R. C. Rodrigues and R. J. L. Lagoa (2008). "A comparative study of alginate beads and an ion-exchange resin for the removal of heavy metals from a metal

plating effluent." Journal of Environmental Science and Health Part a-Toxic/Hazardous Substances & Environmental Engineering **43**(11): 1311-1317.

Silva, T. L., A. Ronix, O. Pezoti, L. S. Souza, P. K. T. Leandro, K. C. Bedin, K. K. Beltrame, A. L. Cazetta and V. C. Almeida (2016). "Mesoporous activated carbon from industrial laundry sewage sludge: Adsorption studies of reactive dye Remazol Brilliant Blue R." Chemical Engineering Journal **303**: 467-476.

Sing, K. S. W., D. H. Everett, R. A. W. Haul, L. Moscou, R. A. Pierotti, J. Rouquerol and T. Siemieniewska (1985). "REPORTING PHYSISORPTION DATA FOR GAS SOLID SYSTEMS WITH SPECIAL REFERENCE TO THE DETERMINATION OF SURFACE-AREA AND POROSITY (RECOMMENDATIONS 1984)." Pure and Applied Chemistry **57**(4): 603-619.

Smidt, E., K. Bohm and M. Schwanninger (2011). "The Application of FT-IR Spectroscopy in Waste Management." Fourier Transforms - New Analytical Approaches and Ftir Strategies: 405-430.

Smith, K. M., G. D. Fowler, S. Pullket and N. J. D. Graham (2009). "Sewage sludge-based adsorbents: A review of their production, properties and use in water treatment applications." Water Research **43**(10): 2569-2594.

Strezov, V. and T. J. Evans (2009). "Thermal processing of paper sludge and characterisation of its pyrolysis products." Waste Management **29**(5): 1644-1648.

Sun, J. C. and H. P. Tan (2013). "Alginate-Based Biomaterials for Regenerative Medicine Applications." Materials **6**(4): 1285-1309.

Tan, X. F., Y. G. Liu, Y. L. Gu, Y. Xu, G. M. Zeng, X. J. Hu, S. B. Liu, X. Wang, S. M. Liu and J. Li (2016). "Biochar-based nano-composites for the decontamination of wastewater: A review." Bioresource Technology **212**: 318-333.

Tay, J. H., X. G. Chen, S. Jeyaseelan and N. Graham (2001). "Optimising the preparation of activated carbon from digested sewage sludge and coconut husk." Chemosphere **44**(1): 45-51.

Veglio, F., A. Esposito and A. P. Reverberi (2002). "Copper adsorption on calcium alginate beads: equilibrium pH-related models." Hydrometallurgy **65**(1): 43-57.

Veksha, A., H. McLaughlin, D. B. Layzell and J. M. Hill (2014). "Pyrolysis of wood to biochar: Increasing yield while maintaining microporosity." Bioresource Technology **153**: 173-179.

Villalobos, P., C. A. Acevedo, F. Albornoz, E. Sanchez, E. Valdes, R. Galindo and M. E. Young (2010). "A BOD monitoring disposable reactor with alginate-entrapped bacteria." Bioprocess and Biosystems Engineering **33**(8): 961-970.

Wang, B., J. Lehmann, K. Hanley, R. Hestrin and A. Enders (2015). "Adsorption and desorption of ammonium by maple wood biochar as a function of oxidation and pH." Chemosphere **138**: 120-126.

Wang, H., B. Gao, S. Wang, J. Fang, Y. Xue and K. Yang (2015). "Removal of Pb(II), Cu(II), and Cd(II) from aqueous solutions by biochar derived from KMnO4 treated hickory wood." Bioresource Technology **197**: 356-362.

Wang, W., Y. Ding, Y. H. Wang, X. S. Song, R. F. Ambrose, J. L. Ullman, B. K. Winfrey, J. F. Wang and J. Gong (2016). "Treatment of rich ammonia nitrogen wastewater with polyvinyl alcohol immobilized nitrifier biofortified constructed wetlands." Ecological Engineering **94**: 7-11.

Wang, Y., Y. Tian, B. Han, H. B. Zhao, J. N. Bi and B. L. Cai (2007). "Biodegradation of phenol by free and immobilized Acinetobacter sp strain PD12." Journal of Environmental Sciences **19**(2): 222-225.

Wang, Y. M., W. J. Tian, C. L. Wu, J. Bai and Y. G. Zhao (2016). "Synthesis of coal cinder balls and its application for CODCr and ammonia nitrogen removal from aqueous solution." Desalination and Water Treatment **57**(46): 21781-21793.

Wannapeera, J., B. Fungtammasan and N. Worasuwannarak (2011). "Effects of temperature and holding time during torrefaction on the pyrolysis behaviors of woody biomass." Journal of Analytical and Applied Pyrolysis **92**(1): 99-105.

Weber, T. W. and R. K. Chakravorti (1974). "PORE AND SOLID DIFFUSION MODELS FOR FIXED-BED ADSORBERS." Aiche Journal **20**(2): 228-238.

Wenjie, Z., W. Dunqiu, K. Yasunori, Y. Taichi, Z. Li and F. Kenji (2008). "PVA-gel beads enhance granule formation in a UASB reactor." Bioresource Technology **99**(17): 8400-8405.

Xu, G. R., X. Yang and L. Spinosa (2015). "Development of sludge-based adsorbents: Preparation, characterization, utilization and its feasibility assessment." Journal of Environmental Management **151**: 221-232.

Yalcin, S., R. Apak and I. Boz (2015). "Enhanced copper(II) biosorption on SiO2-alginate gel composite: A mechanistic study with surface characterization." Korean Journal of Chemical Engineering **32**(10): 2116-2123.

Yang, C., Z. Q. Pang, J. C. Chen and G. H. Yang (2012). PVA-SA immobilized white-rot fungus to treat papermaking wastewater. Material Sciences and Technology, Pts 1 & 2. Y. Li. **560-561:** 672-677.

Yang, Q., Y. Z. Peng, X. H. Liu, W. Zeng, T. Mino and H. Satoh (2007). "Nitrogen removal via nitrite from municipal wastewater at low temperatures using real-time control to optimize nitrifying communities." Environmental Science & Technology **41**(23): 8159-8164.

Yao, H., J. Lu, J. Wu, Z. Y. Lu, P. C. Wilson and Y. Shen (2013). "Adsorption of Fluoroquinolone Antibiotics by Wastewater Sludge Biochar: Role of the Sludge Source." Water Air and Soil Pollution **224**(1).

Yin, C. Y., M. K. Aroua and W. Daud (2007). "Review of modifications of activated carbon for enhancing contaminant uptakes from aqueous solutions." Separation and Purification Technology **52**(3): 403-415.

Yu, L. and Q. Zhong (2006). "Preparation of adsorbents made from sewage sludges for adsorption of organic materials from wastewater." Journal of Hazardous Materials **137**(1): 359-366.

Yue, Z. R., C. L. Mangun and J. Economy (2002). "Preparation of fibrous porous materials by chemical activation 1. ZnCl2 activation of polymer-coated fibers." Carbon **40**(8): 1181-1191.

Zhai, Y. B., X. X. Wei and G. M. Zeng (2004). "Effect of pyrolysis temperature and hold time on the characteristic parameters of adsorbent derived from sewage sludge." Journal of Environmental Sciences **16**(4): 683-686.

Zhai, Y. B., X. X. Wei, G. M. Zeng and D. J. Zhang (2004). "Effects of metallic derivatives in adsorbent derived from sewage sludge on adsorption of sulfur dioxide." Journal of Central South University of Technology **11**(1): 55-58.

Zhai, Y. B., X. X. Wei, G. M. Zeng, D. J. Zhang and K. F. Chu (2004). "Study of adsorbent derived from sewage sludge for the removal of Cd2+, Ni2+ in aqueous solutions." Separation and Purification Technology **38**(2): 191-196.

Zhang, F.-S., J. O. Nriagu and H. Itoh (2005). "Mercury removal from water using activated carbons derived from organic sewage sludge." Water Research **39**(2–3): 389-395.

Zhang, J., M. Liu, T. Yang, K. Yang and H. Y. Wang (2016). "A novel magnetic biochar from sewage sludge: synthesis and its application for the removal of malachite green from wastewater." Water Science and Technology **74**(8): 1971-1979.

Zhang, J. S. and Q. Q. Wang (2016). "Sustainable mechanisms of biochar derived from brewers' spent grain and sewage sludge for ammonia-nitrogen capture." Journal of Cleaner Production **112**: 3927-3934.

Zhang, L. S., W. Z. Wu and J. L. Wang (2007). "Immobilization of activated sludge using improved polyvinyl alcohol (PVA) gel." Journal of Environmental Sciences **19**(11): 1293-1297.

Zhang, W., S. Mao, H. Chen, L. Huang and R. Qiu (2013). "Pb(II) and Cr(VI) sorption by biochars pyrolyzed from the municipal wastewater sludge under different heating conditions." Bioresource Technology **147**: 545-552.

Zhang, Y., Y. F. Li, L. Q. Yang, X. J. Ma, L. Y. Wang and Z. F. Ye (2010). "Characterization and adsorption mechanism of Zn2+ removal by PVA/EDTA resin in polluted water." Journal of Hazardous Materials **178**(1-3): 1046-1054.

Zhong, M., S. Q. Gao, Q. Zhou, J. R. Yue, F. Y. Ma and G. W. Xu (2016). "Characterization of char from high temperature fluidized bed coal pyrolysis in complex atmospheres." Particuology **25**: 59-67.

Zhou, F. S., H. Wang, S. E. Fang, W. H. Zhang and R. L. Qiu (2015). "Pb(II), Cr(VI) and atrazine sorption behavior on sludge-derived biochar: role of humic acids." Environmental Science and Pollution Research **22**(20): 16031-16039.

Zielinska, A. and P. Oleszczuk (2015). "Evaluation of sewage sludge and slow pyrolyzed sewage sludge-derived biochar for adsorption of phenanthrene and pyrene." Bioresource Technology **192**: 618-626.

Zielinska, A. and P. Oleszczuk (2016). "Effect of pyrolysis temperatures on freely dissolved polycyclic aromatic hydrocarbon (PAH) concentrations in sewage sludge-derived biochars." Chemosphere **153**: 68-74.

Appendix

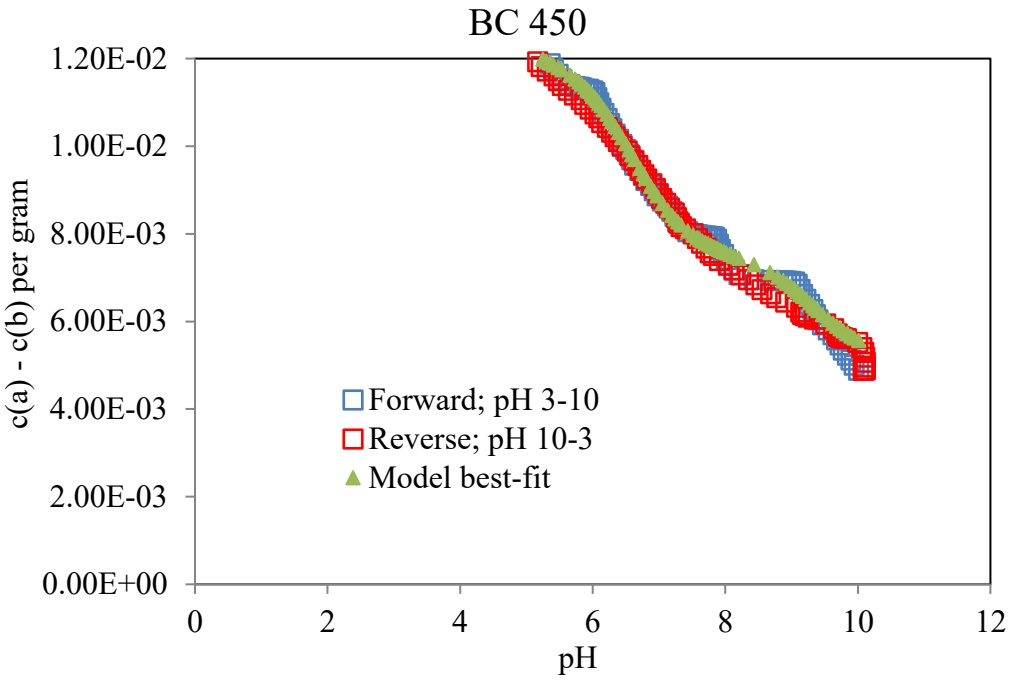

Figure A1: Potentiometric titration of BC 450

Table A1 pKas and site concentrations of 3site models for BC 450

Materials	Sites	pKa_1	pKa_2	pKa_3	Site1 concentration (mol/g)	Site2 concentration (mol/g)	Site3 concentration (mol/g)	Vy
BC450	3	4.35	6.60	9.32	2.67E-04	1.11E-03	15.69E-04	10.06

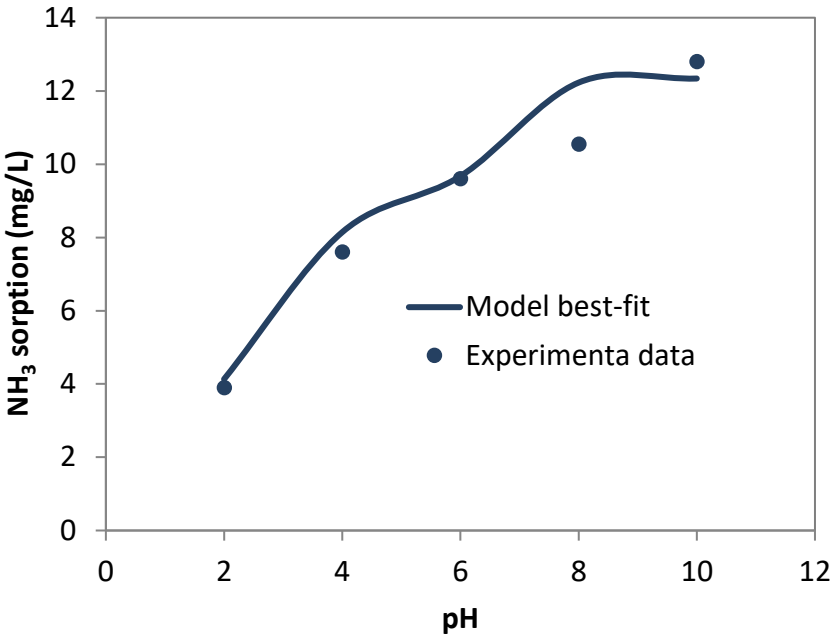

Figure A2: pH edges of ammonia removal from solution by biochar

Table A2: stability constants for ammonia sorb to biochar

Materials	Sites	$logK_{NH4L1}$	$logK_{NH4L2}$	$logK_{NH4H2L2}$	Vy
BC450	2	-0.32	-4.86	3.60	73.25

Table A3: Trace elements of BC 450

	E1 (ppm)	E2 (ppm)
Li	2.1	2
B	10.1	10.1
Na	1428.8	1389.2
Mg	1752.4	1747
Al	3199.6	3031.9
P	6703	6182.6
S	459.1	525.5
K	3954.9	3643.8
Ca	7473.5	6969.4
V	6.2	6.3
Cr	12.3	12.9
Mn	51.4	52.1
Fe	3414.9	3249.9
Co	4.1	4.1

Ni	13.6	13.7
Cu	104.5	104.2
Zn	227.2	228.1
As	1	1
Se	6.2	6.6
Sr	67.9	68.2
Cd	0.6	0.6
Pb	5.9	5.9
U	1	1